

# WHAT DOES THE JOSEPHSON EFFECT TELL US ABOUT THE SUPERCONDUCTING STATE OF THE CUPRATES?

R. Hlubina<sup>1</sup>, M. Grajcar<sup>1</sup>, and E. Il'ichev<sup>2</sup>

<sup>1</sup>Department of Solid State Physics, Comenius University, SK-84248 Bratislava, Slovakia

<sup>2</sup> Institute for Physical High Technology, P.O. Box 100239, D-07702 Jena, Germany

## 1. INTRODUCTION

The defining property of a superconductor is the stiffness of its phase. In conventional low- $T_c$  superconductors this stiffness is so large that in order to directly observe its finite value one has to create a region where it is locally suppressed, the so-called superconducting weak link. The resulting weak link region gives rise to a variety of Josephson effects (for a review, see [1]), in which the superconducting phase becomes a measurable quantity.

In the cuprate superconductors the sensitivity of the Josephson effect to the phase has played a decisive role in establishing a phase-sensitive test of the (now well established) unconventional  $d$ -wave symmetry of their pairing state (for a review, see [2]).

The purpose of this paper which is based on the results of our measurements of the current-phase relation in the cuprates [3, 4, 5, 6] is to argue that besides providing a phase-sensitive test of the pairing symmetry, a quantitative analysis of the Josephson effect in the cuprates provides new insights into the microscopic physics of the cuprates, in particular into the reduced phase stiffness of the cuprates.

Our experiments were carried out on two types of Josephson junctions: [001] tilt grain boundary junctions [3, 4, 6] and  $c$ -axis junctions between a cuprate and a low- $T_c$  superconductor [5]. Let us start with a brief discussion of these two types of junctions.

1. Grain boundary junctions have been studied since the very beginning of the cuprate

research (for a review see [7]). In particular, it has been realized very early on that grain boundaries are *the* current limiting element of polycrystalline materials and as such are to be avoided in large current applications. However, after having been used in the phase sensitive experiments [2], the situation changed completely when it was realized that cuprate grain boundary junctions might form the basis of a completely new type of superconducting electronics, based on the use of the so-called  $\pi$ -junctions.

In an idealized picture, a grain boundary junction can be thought of as a planar interface of two grains. The junction is characterized by two angles  $\theta_1$  and  $\theta_2$  between the normal to the interface and the crystallographic axes in the grains, see Fig. 1.

It is an experimental fact that the junction transparency  $\mathcal{D}$  depends predominantly on the misorientation angle  $\theta = \theta_2 - \theta_1$ . The microstructure of the grain boundary is quite complicated and at the moment there exists no generally accepted picture of it. In this paper we adopt the point of view advocated by Hilgenkamp and Mannhart [7], who view the junction as a locally underdoped (and insulating) region. The width of this insulating barrier is supposed to be proportional to  $\theta$ , therefore leading quite naturally to the experimentally observed scaling  $\mathcal{D}(\theta) = \exp(-\theta/\theta_0)$  with  $\theta_0 \approx 5^\circ$ . In this paper we shall be concerned mostly with grain boundary junctions with misorientation angle  $\theta = 45^\circ$  for which  $\mathcal{D} \approx e^{-9} \approx 10^{-4}$ .

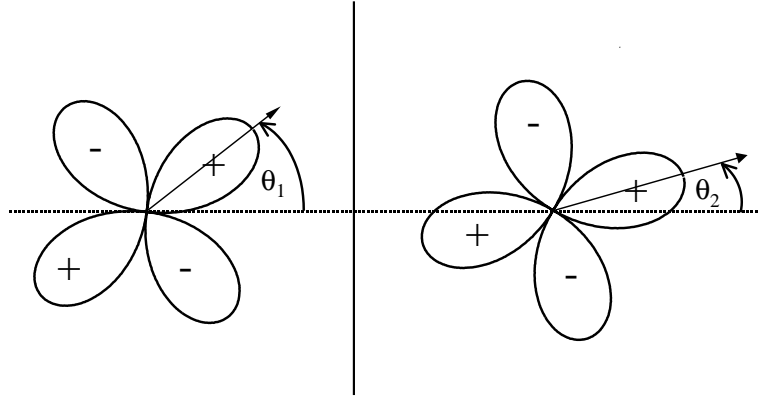


Figure 1: Schematic drawing of a [001] tilt grain boundary junction.

We believe that grain boundary junctions with  $\theta > \theta_0$  are to be described as featureless junctions in the tunnel limit. An alternative explanation of the very small transmission probability  $\mathcal{D}(\theta)$  could invoke the presence of pinholes in the barrier, whose density would decrease exponentially with  $\theta$ . We believe that measurements [6, 8] of the relation between the superconducting current  $I$  and the phase difference  $\varphi$  across the junctions with  $\theta = 24^\circ$  and  $36^\circ$  have ruled out this possibility, since the results were fully consistent with the tunnel limit prediction  $I(\varphi) \propto \sin \varphi$  and no trace of higher harmonics indicative of small barrier weak links were found, see Fig. 2.

2. The other type of junctions whose current-phase relation we have studied are the so-called  $c$ -axis junctions between the cuprates and low- $T_c$  superconductors. In this type

of junctions the interface is parallel to the  $\text{CuO}_2$  planes and the current flows along the  $c$  axis of the cuprates. Because of the layered structure of the cuprates the interlayer forces are presumably much weaker than those within the layers, and therefore much cleaner and better defined interfaces are to be expected for this type of junctions, when compared with the grain boundary junctions.

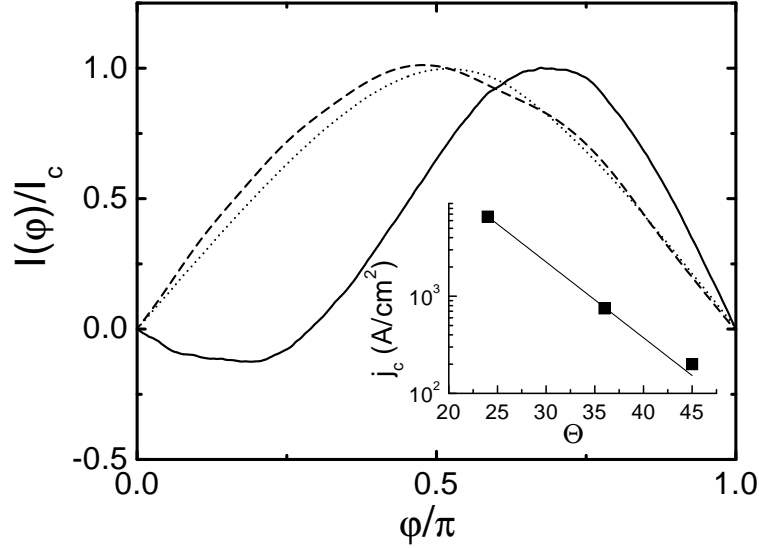


Figure 2: Current-phase relation at  $T = 15$  K for symmetric GBJJs with  $\theta = 24^\circ$  (dotted line),  $36^\circ$  (dashed line) and  $45^\circ$  (solid line). The inset shows the scaling  $j_c \propto \exp(-\theta/\theta_0)$  of the critical current density with  $\theta_0 = 5.6^\circ$ . Taken from [6].

## 2. THEORY

**2.1. GRAIN BOUNDARY JUNCTIONS.** Our main interest in this paper regards the current-phase relation  $I(\varphi)$ , which is on general grounds assumed to be a  $2\pi$  periodic function. Moreover, in absence of magnetic fields we expect that  $I(-\varphi) = -I(\varphi)$  and therefore we can write [1]

$$I(\varphi) = I_1 \sin \varphi + I_2 \sin 2\varphi + \dots \quad (1)$$

The  $d$ -wave symmetry of the pairing state in the cuprates requires that odd harmonics  $I_1, I_3, \dots$  change sign with  $\theta_i \rightarrow \theta_i + \pi/2$ . If we keep only the lowest-order angular harmonics, we can therefore write [9]

$$I_1 = I_c \cos 2\theta_1 \cos 2\theta_2 + I_s \sin 2\theta_1 \sin 2\theta_2. \quad (2)$$

The coefficients  $I_c, I_s$  are functions of the barrier strength, temperature  $T$ , etc. In particular, if the tunneling is allowed only for a narrow range of impact angles around normal incidence, only the  $I_c$  term survives. This situation has been considered in the early paper

by Sigrist and Rice [10], who suggested to use the first term of Eq. 2 as a simple approximate formula which respects the symmetries of the Ambegaokar-Baratoff like expression (at  $T = 0$ ) for the critical current,

$$\frac{\pi \Delta_k \Delta_q}{e R_N (|\Delta_k| + |\Delta_q|)} K \left( \frac{|\Delta_k - \Delta_q|}{|\Delta_k| + |\Delta_q|} \right) \rightarrow I_c \cos 2\theta_1 \cos 2\theta_2, \quad (3)$$

where  $R_N$  is the resistance of the junction in the normal state,  $\Delta_k, \Delta_q$  are gap functions for the case of normal incidence in the two superconducting electrodes, and  $K$  is the complete elliptic integral.

On the other hand, the even harmonics  $I_2, I_4, \dots$  are not forced by symmetry to change sign and therefore we neglect their weak angular dependence (except for the strong dependence on the barrier transparency  $\mathcal{D}(\theta)$ ). This then implies (as first noted in [11]) that for the so-called asymmetric  $45^\circ$  grain boundary junctions (i.e.  $\theta_1 = 45^\circ, \theta_2 = 0^\circ$ ), the first harmonic  $I_1$  vanishes by symmetry and the current-phase relation can be approximated by  $I(\varphi) = I_2 \sin 2\varphi$ .

In real life the junction interface meanders around its mean (nominal) direction. In that case we wish to interpret the function  $I_1(\theta_1, \theta_2)$  as a relation between the local critical current density and the local interface geometry. Structural studies of grain boundaries [12] show that the interface is typically faceted with a typical size of a facet  $\approx 100$  nm. Since this length scale is much larger than both relevant electronic length scales, the Fermi wavelength and the coherence length, we believe that the macroscopic first harmonic can be estimated by a simple averaging of Eq. 2 along the interface. Making use of such a procedure, if the local junction geometry is described by  $\theta_i + \chi(x)$ ,  $I_1$  of a rough interface is given by [6]

$$I_1 = \frac{1}{2}(I_c + I_s) \cos 2\theta + \frac{x}{2}(I_c - I_s) \cos 2(\theta_1 + \theta_2), \quad (4)$$

where  $x = \langle \cos 4\chi \rangle$  is an interface roughness parameter and  $\langle \dots \rangle$  denotes an average along the interface. Note that in the completely rough limit  $x = 0$ ,  $I_1$  depends only on the misorientation angle  $\theta$  and not on the individual angles  $\theta_i$  [2], since in that limit the notion of the direction of the interface is meaningless.

On the other hand, since  $I_2$  is not forced by symmetry to depend strongly on  $\theta_i$  (except for the dependence through the barrier transmission on the misorientation angle  $\theta$ ), we expect that  $I_2$  will exhibit only a weak dependence on the surface roughness  $x$ .

Summarizing the above symmetry arguments, it follows that  $d$ -wave symmetry and sufficient interface roughness (small  $x$ ) imply enhanced  $I_2/I_1$  ratios for all  $45^\circ$  junctions.

However, while very robust, the symmetry arguments do not provide estimates of the ratio  $I_2/I_1$ . In what follows we attempt a more quantitative analysis of the Josephson effect. The increased level of detail has its prize, however: we have to introduce a microscopic model of the junction. Two such models have been discussed in the literature: a perfectly flat interface which leads to the presence of midgap states in the case of an impenetrable barrier [13], and a model emphasizing the roughness of the interface and the subsequent development of a nontrivial pattern of currents flowing along the interface [14].

**2.1.1. IDEALLY FLAT JUNCTIONS.** Let us consider first the ‘flat’ scenario. The key

role in this approach is played by the concept of the so-called midgap states, which should form at surfaces of anomalous superconductors. Theory predicts that the number of midgap states should be maximal for (110)-like surfaces of  $d$ -wave superconductors and no such states should form at (100) and (001)-like surfaces [13]. The presence (and the nontrivial surface orientation dependence) of such midgap states in the cuprates is well documented by now by STM spectroscopy [15] and by grain boundary tunneling spectroscopy [16]. It has been also suggested that such bound states are at the origin of the observed nonmonotonic temperature dependence of the penetration depth [17].

Let us turn now to the study of the influence of the midgap states on the Josephson effect in the cuprates, following the early proposal of Tanaka and Kashiwaya [18] (for reviews, see [19, 20]). Within the simplest description, we consider a circular Fermi line, specular reflection at the interface, and a constant order parameter in the superconducting grains. Because of the translational symmetry along the junction, the scattering problem factorizes into a set of independent problems for each given impact angle.

The energy of the Andreev bound states is governed by the probability  $D(\theta, \vartheta)$  of transmission for impact angle  $\vartheta$ . The function  $D(\theta, \vartheta)$  depends on the details of the barrier, such as its width and height, none of which are known reliably in the present context. The only direct experimental measure of the barrier transmission is the resistance per square of the junction in the normal state,  $R_{\square} = (h/2e^2)(\pi d/k_F \mathcal{D})$ , which provides us with one moment of the function  $D(\theta, \vartheta)$ ,  $\mathcal{D}(\theta) = \int_0^{\pi/2} d\vartheta \cos \vartheta D(\theta, \vartheta)$ .

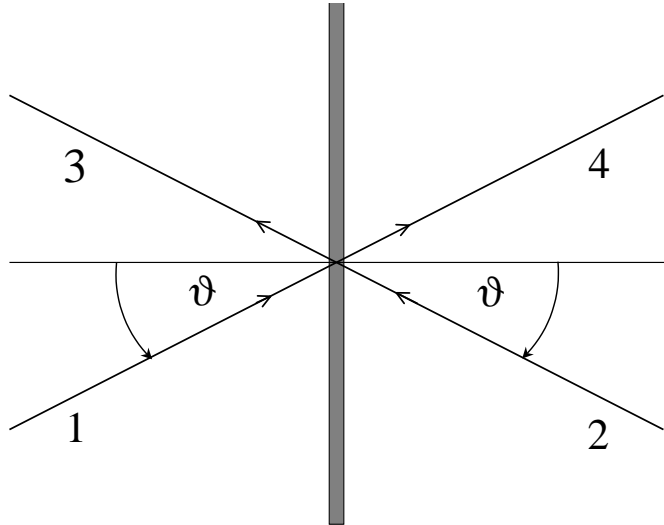


Figure 3: Trajectories of the particles for specular reflection on a flat junction interface. The impact angle  $\vartheta$  is the same for both sides of the junction.

Let us calculate the energy of the Andreev bound state corresponding to the incoming (outgoing) trajectories in the left and right grains denoted 1 and 2 (3 and 4), respectively (see Fig. 3). To this end, let us denote the order parameter on the trajectory  $i$  as  $\Delta_i = |\Delta_i|S_i$ , where  $S_i = \pm 1$  is the sign. The qualitative character of the bound state depends on the relative value of the signs  $S_i$ .

Before proceeding, let us recall that for an impenetrable barrier with  $D \rightarrow 0$ , a midgap state is formed in the left (right) grain for  $S_1 = -S_3$  ( $S_2 = -S_4$ ), i.e. when the sign of

$\Delta$  changes under reflection at the interface [13]. In the tunnel limit, the energy of the Andreev bound state can belong to one of the following three classes:

(i) The signs of  $\Delta$  change under reflection on both sides of the junction,  $S_1 = -S_3$  and  $S_2 = -S_4$ . In that case the two midgap states on both sides of the junction are split by the finite value of  $D$  [21]:

$$\varepsilon(\theta, \vartheta, \varphi) = \pm \sqrt{\frac{4D(\theta, \vartheta)|\Delta_1\Delta_2\Delta_3\Delta_4|}{(|\Delta_1| + |\Delta_3|)(|\Delta_2| + |\Delta_4|)}} \sqrt{\frac{1 - S_1S_2 \cos \varphi}{2}}. \quad (5)$$

Note that  $\varepsilon \propto \sqrt{D}$ , as is usual for degenerate perturbation theory.

(ii) The midgap state is formed only on one side of the junction, the left one for definiteness ( $S_1 = -S_3$ ,  $S_2 = S_4$ ). In that case there is only one anomalous Andreev bound state, [21]:

$$\varepsilon(\theta, \vartheta, \varphi) = D(\theta, \vartheta) \frac{|\Delta_1\Delta_3|}{|\Delta_1| + |\Delta_3|} S_1S_2 \sin \varphi. \quad (6)$$

(iii) There are no midgap states on both sides of the junction, i.e.  $S_1 = S_3$  and  $S_2 = S_4$ . In this case there are no anomalous Andreev bound states and the junction resembles qualitatively that between two  $s$ -wave superconductors. Note that this type of processes is always realized for  $\vartheta = 0^\circ$ .

Once the quasiparticle energies are known, the free energy due to Andreev levels per unit area of the junction reads

$$F_\square^A(\varphi) = -\frac{k_F T}{2\pi d} \sum_n \int_{-\pi/2}^{\pi/2} d\vartheta \cos \vartheta \ln \left[ 1 + \exp \left( -\frac{\varepsilon_n(\vartheta)}{T} \right) \right], \quad (7)$$

where  $d$  is the average distance between the  $\text{CuO}_2$  planes and the index  $n$  numerates all  $\varphi$ -dependent energy levels for the impact angle  $\vartheta$ . According to general principles, the current-phase relation  $I(\varphi)$  can be determined from the  $\varphi$ -dependence of the total junction free energy,  $I = (2\pi/\Phi_0)\partial F/\partial \varphi$  and the density of supercurrent across the junction reads  $j(\varphi) = (2\pi/\Phi_0)\partial F_\square/\partial \varphi$ . We emphasize that it is the total  $\varphi$ -dependent free energy density  $F_\square(\varphi)$  (and not only the contribution of the Andreev bound states  $F_\square^A$ ) which determines  $j(\varphi)$ .

Before proceeding we should like to point out that, in general, a finite phase difference  $\varphi$  across the junction leads to a nonzero current along the junction [22]. This current generates a magnetic field which has to be screened by the Meissner currents in the superconducting electrodes [23], thus leading to an additional term in the free energy,  $F_\square^M(\varphi)$ .

The spontaneously generated current along the interface can be calculated as follows. Since all four momenta involved in interface scattering with impact angle  $\vartheta$  (see Fig. 3) have the same momentum  $k_y$  along the junction, the  $y$  component of the current density carried by the Andreev bound state with energy  $\varepsilon(\vartheta)$  is

$$j_y(\vartheta, x) = \frac{e\hbar k_y}{m} (|u(x, \vartheta)|^2 + |v(x, \vartheta)|^2),$$

where  $u(x)$  and  $v(x)$  are the two components of the Andreev level wavefunction. Since  $u(x), v(x)$  decay exponentially on the distance  $\sim \xi$  from the interface (where  $\xi \sim \hbar v_F/\Delta$

is the coherence length), also the net current along the interface

$$j_y(x) = \frac{k_F L}{2\pi} \sum_n \int_{-\pi/2}^{\pi/2} d\vartheta \cos \vartheta j_y(\vartheta, x) f(\varepsilon_n(\vartheta)) \quad (8)$$

is localized within  $\xi$  from the interface. From Eq. 8 it follows that the linear density of the total current flowing along the grain boundary per  $\text{CuO}_2$  layer,  $J_0 = \int_{-\infty}^{\infty} j_y(x)$ , is

$$J_0 = \frac{e\varepsilon_F}{\hbar d} \sum_n \int_{-\pi/2}^{\pi/2} \frac{d\vartheta}{2\pi} \sin 2\vartheta f(\varepsilon_n(\vartheta)), \quad (9)$$

where  $\varepsilon_F$  is the Fermi energy. In deriving Eq. 9 we have made use of the fact that the Andreev level wavefunctions are normalized,  $\int_{-\infty}^{\infty} dx (|u(x)|^2 + |v(x)|^2) = (Ld)^{-1}$ .

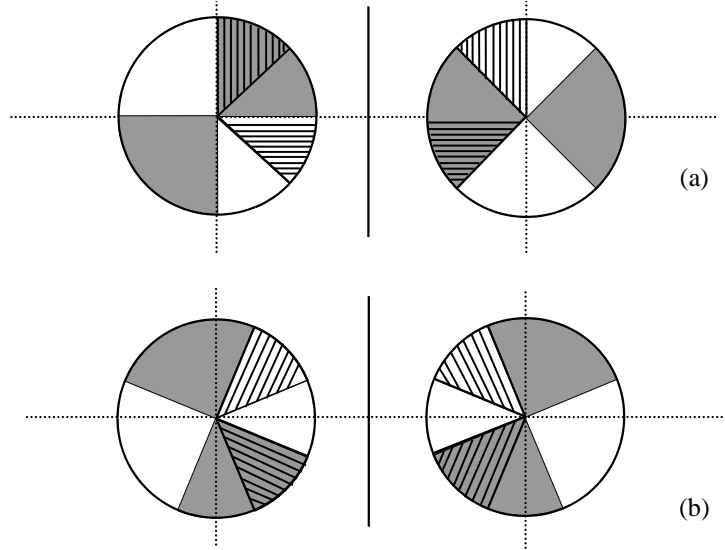


Figure 4: Schematic drawings of asymmetric (a) and symmetric (b)  $45^\circ$  grain boundary junctions. Shaded regions correspond to a positive order parameter. For asymmetric junctions, impact angles for which  $S_1 S_2 = -1$  are denoted by the hatched regions. For symmetric junctions the hatched regions correspond to trajectories with midgap states on both sides of the junction.

*Asymmetric  $45^\circ$  junctions.* In what follows, let us apply the above formalism to the two special cases of interest to us, namely the asymmetric and symmetric  $45^\circ$  junctions. For asymmetric junctions, the trajectories for all impact angles are of type (ii), see Fig. 4. Since in this case  $\Delta_1(\vartheta) = -\Delta_3(\vartheta) = \Delta \sin 2\vartheta$  and  $\Delta_2(\vartheta) = \Delta_4(\vartheta) = \Delta \cos 2\vartheta$ , the energy of the Andreev levels is

$$\varepsilon(\vartheta) = \frac{\Delta}{2} D(\vartheta) |\sin 2\vartheta| \text{sign}(\sin 4\vartheta) \sin \varphi.$$

For the sake of simplicity we consider a simple model for the barrier transmission function,  $D(\vartheta) = D(0)$  for  $|\vartheta| < \vartheta_0 < \pi/4$  and  $D(\pi/4) \ll D(0)$  otherwise. In this case  $\mathcal{D} \approx$

$D(0) \sin \vartheta_0$  and the typical energy of the bound states  $\sim \mathcal{D}\Delta$  sets the energy scale of the problem. In the two extreme limits  $T \ll \mathcal{D}\Delta$  and  $T \gg \mathcal{D}\Delta$ , respectively, we find

$$\begin{aligned} F_{\square}^A &= -\frac{\vartheta_0}{4\pi} \frac{k_F \mathcal{D}\Delta}{d} |\sin \varphi|, \\ F_{\square}^A &= \frac{\vartheta_0}{48\pi} \frac{k_F \mathcal{D}^2 \Delta^2}{Td} \cos 2\varphi. \end{aligned} \quad (10)$$

From Eq. 9 it follows that  $J_0$  depends only on the population of the Andreev levels. Let us for definiteness consider the case  $\varphi > 0$ . Depending on the impact angle  $\vartheta$ , the trajectories can be classified into two distinct groups: The hatched regions in Fig. 4 correspond to  $S_1 S_2 = -1$ , whereas for the remaining trajectories  $S_1 S_2 = 1$ . Thus the energy of the Andreev levels in the hatched (not hatched) regions is negative (positive). Therefore at  $T = 0$  only the Andreev levels in the hatched regions are occupied and from Eq. 9 we find  $J_0 = 0$ . This effect has been called superscreening in the literature [24]. At finite temperatures  $T \gg D(\pi/4)\Delta$  an explicit calculation leads to a finite current along the junction,

$$J_0 = -\frac{\vartheta_0^2}{4\pi} \frac{ek_F v_F}{d} \frac{\mathcal{D}\Delta \sin \varphi}{3T + \mathcal{D}\Delta |\sin \varphi|}.$$

The surface currents due to the Andreev bound states generate magnetic fields which have to be screened by the Meissner currents in the superconducting grains. As pointed out in [25], this leads to an increase of the total junction energy, whose magnitude we now estimate in the simple case of a two dimensional interface (in the  $y$ - $z$  plane) between 3D superconducting grains. Of course, most experiments are carried out on thin films and thus the 3D geometry is not fully appropriate. However, since the film thicknesses are typically  $\sim 1000 \text{ \AA}$  which is comparable to the bulk penetration depth, our estimates should remain qualitatively correct.

Since the current due to Andreev bound states flows on scale  $\xi$ , we model its distribution as  $\mathbf{j} = (0, j, 0)$  with  $j(x) = J_0 \delta(x)$ . Within the London theory (assuming bulk penetration depth  $\lambda$ ), the distribution of the Meissner current and of the magnetic field can be readily calculated and the results are shown in Fig. 5. The sum of the energy of the magnetic field and of the kinetic energy of the superflow (per unit area of the interface) is easily seen to be  $F_{\square}^M = \mu_0 J_0^2 \lambda / 4$ .

Therefore the  $\varphi$ -dependent part of the total free energy density  $F_{\square}(\varphi) = F_{\square}^A(\varphi) + F_{\square}^M(\varphi)$  for  $T \ll \mathcal{D}\Delta$  and  $T \gg \mathcal{D}\Delta$  reads

$$\begin{aligned} F_{\square}(\varphi) &= \frac{\vartheta_0}{4\pi} \frac{k_F}{d} \Delta \left[ -\mathcal{D} |\sin \varphi| + \frac{\vartheta_0^3}{8} \frac{\xi}{\lambda} \left( \frac{\sin \varphi}{|\sin \varphi| + \alpha} \right)^2 \right], \\ F_{\square}(\varphi) &= \frac{\vartheta_0}{48\pi} \frac{k_F}{d} \frac{\mathcal{D}^2 \Delta^2}{T} \left[ 1 - \frac{\vartheta_0^3}{12} \frac{\hbar v_F / T}{\lambda} \right] \cos 2\varphi, \end{aligned} \quad (11)$$

respectively, where  $\xi = \hbar v_F / \Delta$  and  $\alpha = 3T / \mathcal{D}\Delta$ . Several points regarding Eq. 11 are to be stressed. First, in the low temperature limit, our result agrees qualitatively with [25] in that the free energy is minimized for  $\varphi = 0$  or  $\varphi = \pi$ , if  $\mathcal{D} \ll \vartheta_0^3 \xi / \lambda$  (i.e. the bound state energy gain is smaller than the Meissner energy loss). In the opposite limit when the bound state energy dominates  $F_{\square}$ , the free energy is minimized for  $\varphi = \pm \pi/2$ .



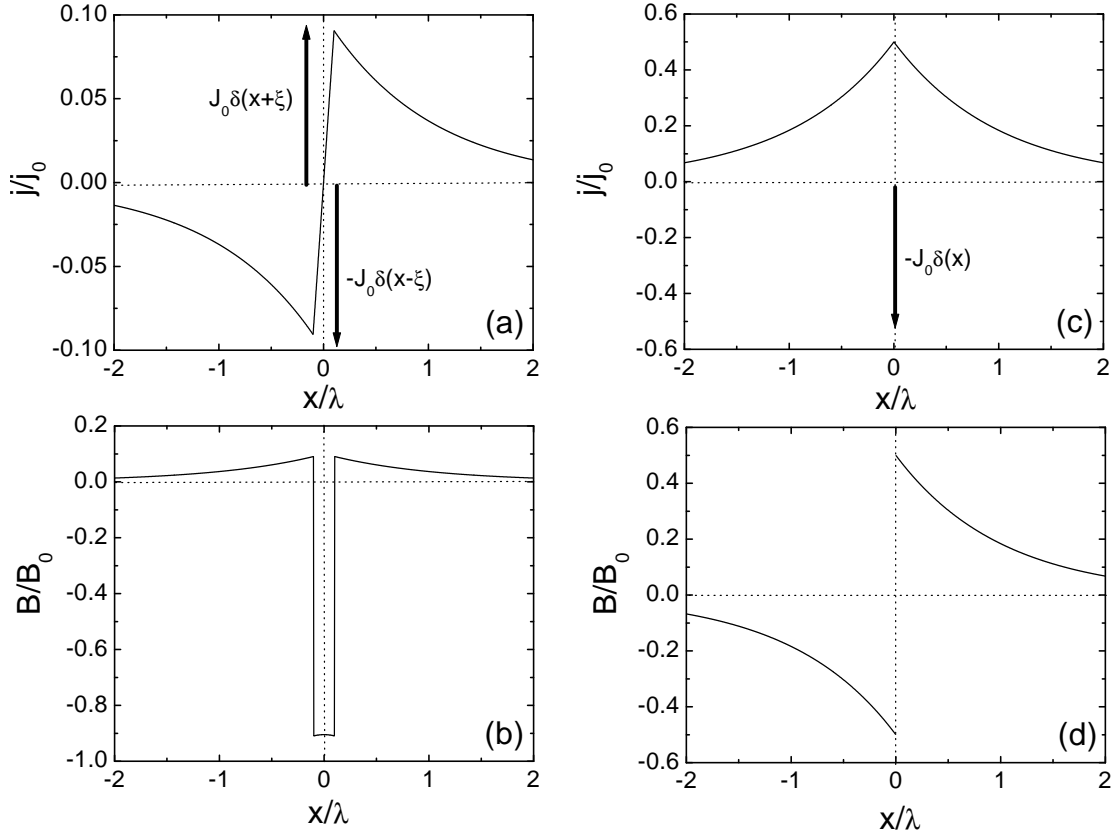


Figure 5: The distribution of supercurrent density (a) in units of  $j_0 = J_0/\lambda$  and magnetic field (b) in units of  $B_0 = \mu_0 J_0$  for symmetric  $45^\circ$  grain boundary junctions. (c,d): the same for asymmetric  $45^\circ$  junctions. In all figures we have used  $\xi/\lambda = 0.1$ .

From the normal state resistivity of  $45^\circ$  junctions we estimate  $\mathcal{D} \sim 10^{-4}$ . If we take  $\xi \approx 30 \text{ \AA}$  and  $\lambda \approx 1500 \text{ \AA}$  relevant for the cuprates, we estimate that for not too strongly angle dependent tunneling, the Meissner energy should dominate  $F_\square$  at low temperatures. We should like to point out that by no means this implies trivial physics. Just on the contrary, as shown in Fig. 6, dominant Meissner energy leads to a doubled periodicity of  $I(\varphi)$ . This is qualitatively similar to the well studied case when  $F_\square^A$  dominates. However, there are two major qualitative differences with respect to the case of dominant bound state energy: (i) the (degenerate) ground state corresponds to a state when no currents flow along the junction, and (ii) the current-phase relation becomes steep in the minima (not maxima) of the junction energy, see Fig. 6.

At temperatures above the bound state energy  $\mathcal{D}\Delta$  (which is presumably the case down to helium temperatures due to the small value of  $\mathcal{D}$ ), we find  $F_\square \propto \cos 2\varphi$  leading to

$$j(\varphi)R_\square = -\frac{\pi\vartheta_0}{12} \frac{\mathcal{D}\Delta^2}{eT} \left[ 1 - \frac{\vartheta_0^3 \hbar v_F/T}{12 \lambda} \right] \sin 2\varphi. \quad (12)$$

A pure second harmonic is seen to develop, in complete agreement with the symmetry analysis. Note that in this temperature range the Meissner contribution to  $I(\varphi)$  becomes

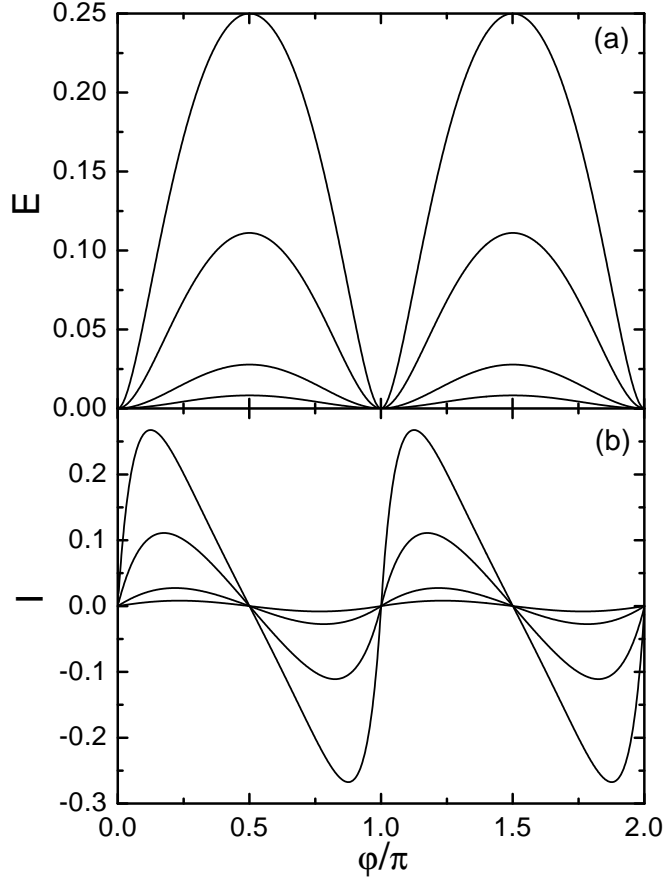


Figure 6: (a) Meissner energy  $F^M$  of an asymmetric  $45^\circ$  junction (in arbitrary units) as a function of the phase difference  $\varphi$  across the junction. (b) Superconducting current  $I = (2\pi/\Phi_0)\partial F^M/\partial\varphi$  (in arbitrary units) as a function of  $\varphi$ . In both figures  $\alpha = 1, 2, 5, 10$  from top to bottom.

negligible. This is a result of the thermal fluctuations which reduce the surface current  $J_0$  severely.

*Symmetric  $45^\circ$  junctions*, i.e. junctions with  $\theta_1 = -\theta_2 = 22.5^\circ$ . In this case, trajectories with impact angles in the hatched regions of Fig. 4 are of type (i), whereas the remaining ones are of type (iii). As a function of the impact angle, the gap functions can be written  $\Delta_1(\vartheta) = \Delta_2(\vartheta) = \Delta \cos(2\vartheta - \pi/4)$  and  $\Delta_3(\vartheta) = \Delta_4(\vartheta) = \Delta \cos(2\vartheta + \pi/4)$ . Again we have to make an assumption about the dependence of the transparency on the impact angle. We start by considering the case of a weakly dependent  $D(\vartheta)$ . As a rough approximation, we approximate all Andreev levels of type (iii) by their value for  $\vartheta = 0^\circ$  [21], and all levels of type (i) by the  $\vartheta = 45^\circ$  case,

$$\begin{aligned}\varepsilon(0, \varphi) &= \pm 2^{-1/2} \Delta \sqrt{1 - D(0) \sin^2(\varphi/2)}, \\ \varepsilon(\pi/4, \varphi) &= \pm 2^{-1/2} \Delta \sin(\varphi/2) \sqrt{D(\pi/4)},\end{aligned}$$

where we assume that  $D(\pi/4) < D(0) \ll 1$ . Note that for every impact angle  $\vartheta$  there exist two levels with energies  $\pm\varepsilon(\vartheta)$ . Therefore  $\sum_n f(\varepsilon_n(\vartheta)) = 1$  and the integral Eq. 9

vanishes. In other words, the total supercurrent along the interface vanishes by symmetry. This does not mean, however, that no currents are flowing along the interface. In order to estimate the Meissner contribution to the interface free energy  $F_{\square}^M$ , we model the current distribution generated by the Andreev levels as  $j(x) = J_0[\delta(x + \xi) - \delta(x - \xi)]$  where  $\xi$  is the coherence length and  $J_0 = \int_0^\infty dx j_y(x)$ . The resulting magnetic field and the Meissner screening currents can be calculated within the London theory in a similar way as for the asymmetric junctions (see Fig. 5) and the resulting contribution to the junction free energy is  $F_{\square}^M = \mu_0 J_0^2 \xi$ . Note that  $F_{\square}^M$  is reduced with respect to the case of asymmetric junctions (if we assume the same value of  $J_0$  in both cases) by a factor  $4\xi/\lambda \ll 1$ , since it arises from a higher order moment of the current distribution  $j_y(x)$ . Due to this small factor,  $F_{\square}^M/F_{\square}^A \sim (\xi/\lambda)^2/D$  even if we take the maximal possible value of  $J_0$ ,  $J_0 \sim ek_F v_F/d$ . Therefore the Meissner contribution to the interface free energy will be neglected and the Josephson current is calculated from

$$j(\varphi) = \frac{2\pi}{\Phi_0} \frac{\partial F_{\square}^A}{\partial \varphi} = \frac{k_F}{\Phi_0 d} \sum_n \int_{-\pi/2}^{\pi/2} d\vartheta \cos \vartheta f(\varepsilon_n(\vartheta)) \frac{\partial \varepsilon_n}{\partial \varphi}. \quad (13)$$

This implies that  $j(\varphi) = j_n(\varphi) + j_a(\varphi)$ , where the normal and anomalous contributions are, respectively:

$$\begin{aligned} j_n(\varphi) &= \frac{\pi k_F \Delta}{8 \Phi_0 d} \frac{D(0) \sin \varphi}{2^{3/2} \sqrt{1 - D(0) \sin^2(\varphi/2)}} \tanh \frac{\Delta \sqrt{1 - D(0) \sin^2(\varphi/2)}}{2^{3/2} T}, \\ j_a(\varphi) &= -\frac{\pi k_F \Delta}{8 \Phi_0 d} \cos(\varphi/2) \sqrt{D(\pi/4)} \tanh \frac{\Delta \sin(\varphi/2) \sqrt{D(\pi/4)}}{2^{3/2} T}. \end{aligned} \quad (14)$$

At intermediate temperatures  $\Delta \sqrt{D(\pi/4)} \ll T \ll \Delta$  the anomalous (normal) Andreev levels are in the high (low) temperature limit. Therefore Eq. 14 simplifies considerably and the first two harmonics of  $j(\varphi)$  can be written as

$$\begin{aligned} \frac{j_1}{j_L} &= D(0) - \frac{\Delta}{2T} D(\pi/4), \\ \frac{j_2}{j_L} &= -\frac{1}{8} D(0)^2 - \frac{1}{24} \left( \frac{\Delta}{2T} \right)^3 D(\pi/4)^2, \end{aligned} \quad (15)$$

where  $j_L = (\pi/16\sqrt{2})k_F \Delta/\Phi_0 d$  is comparable with the bulk depairing current density. Thus, for weakly angle-dependent tunneling and above the energy of anomalous Andreev levels, theory predicts a sign change of the first harmonic at a temperature  $T^* = \Delta D(\pi/4)/2D(0)$  and a second harmonic monotonically increasing with decreasing temperature.

In the opposite limit of a peaked barrier transparency  $D(\vartheta) = D(0) \exp(-\vartheta/\vartheta_0)$ , the junction is equivalent to a symmetric junction between  $s$ -wave superconductors with order parameters  $\Delta/\sqrt{2}$ . Therefore the current-phase relation in the  $T \rightarrow 0$  and  $T \rightarrow T_c$  limits, respectively, reads

$$j(\varphi) R_{\square} = \frac{\pi}{2\sqrt{2}} \frac{\Delta}{e} \left[ \sin \varphi - \frac{D(0)}{16} \sin 2\varphi \right],$$

$$j(\varphi)R_{\square} = \frac{\pi \Delta^2}{8 eT} \left[ \sin \varphi - \frac{D(0)}{48} \left( \frac{\Delta}{2T} \right)^2 \sin 2\varphi \right]. \quad (16)$$

Unlike Eq. 15, the result Eq. 16 predicts a monotonically increasing first harmonic with decreasing temperature.

**2.2. *c*-AXIS JUNCTIONS.** Let us briefly discuss the supercurrent in *c*-axis junctions between  $\text{YBa}_2\text{Cu}_3\text{O}_x$  (YBCO) and low- $T_c$  superconductors [5]. In YBCO the dominant component of the superconducting order parameter has *d*-wave symmetry [2]. However, due to the orthorhombic structure of YBCO, a finite component with *s*-wave symmetry is admixed to the dominant *d*-wave order parameter. The in-plane phase sensitive experiments imply that the *d*-wave component remains coherent through the whole sample [2], while an elegant *c*-axis tunneling experiment shows directly that the *s*-wave order parameter component does change sign across the twin boundary [26].

The above picture of the YBCO pairing state is challenged by the experimental observation of a finite *c*-axis Josephson current between heavily twinned YBCO and a Pb counterelectrode [27]. Namely, the contribution of the *s*-wave part of the YBCO order parameter to the Josephson coupling between a conventional superconductor (superconductor with a pure *s*-wave symmetry of the order parameter, for example Pb or Nb) and YBCO should average to zero for equal abundances of the two types of twins in YBCO. In other words, the macroscopic pairing symmetry of twinned YBCO samples should be a pure *d*-wave [9]. Tanaka has shown that a finite second order Josephson current obtains for a junction between the *s*-wave and *c*-axis oriented pure *d*-wave superconductors [11]. However, measurements of microwave induced steps at multiples of  $hf/2e$  on the *I-V* curves of Pb/Ag/YBCO tunnel junctions imply dominant first order tunneling [28]. Therefore the finite *c*-axis Josephson current has to result from a nonvanishing admixture of the *s*-wave component to the macroscopic order parameter of YBCO [9]. Two alternatives of how this can take place in the junctions based on twinned YBCO have been discussed in the literature:

(i) Sigrist *et al.* have suggested that the phase of the *s*-wave component in YBCO does not simply jump from 0 to  $\pi$  upon crossing the twin boundary, but rather changes in a smooth way, attaining the value of  $\pi/2$  right at the twin boundary [29]. The twinned YBCO sample is thus assumed to exhibit a macroscopic *d + is* pairing symmetry. A related picture has been proposed by Haslinger and Joynt, who suggest a *d + is* surface state of YBCO [30].

(ii) A difference in the abundances of the two types of twins implies a *d + s* symmetry of the macroscopic pairing state [31]. It has been pointed out [5] that also structural peculiarities of other type (such as a lamellar structure in a preferred direction) may lead to the *d + s* macroscopic pairing symmetry.

The primary motivation of our experiment [5] was to determine which of the above two scenaria is realized in YBCO. In what follows we will show that this question can be conveniently answered by measuring the relative sign of the first two harmonics of  $I(\varphi)$ . Let us consider first the *d + s* scenario. As will be shown explicitly in Eqs. 31, 32, in this case the junction free energy can be written

$$F(\varphi) = -F_1 \cos \varphi + F_2 \cos 2\varphi \quad (17)$$

with  $F_1, F_2 > 0$ . As shown in Fig. 7, this choice of signs corresponds to a free energy which is flat (curved) close to the minima (maxima). In terms of the current phase relation, this case corresponds to the usual case when  $I(\varphi)$  is steep in the vicinity of  $\pm\pi$ , as in the Kulik-Omelyanchuk theory [1].

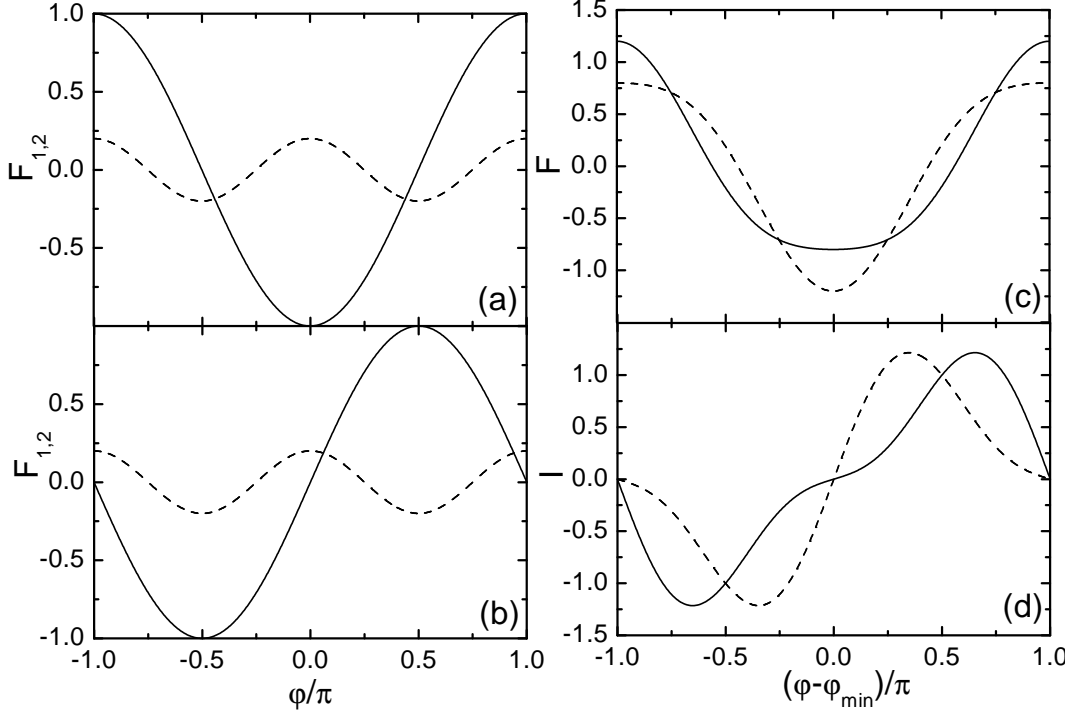


Figure 7: (a,b): Schematic drawing of the contributions from the first (solid lines) and second (dashed lines) harmonics to the free energy of  $c$ -axis junctions between a conventional superconductor and YBCO for various macroscopic pairing states in YBCO. (a):  $d+s$  pairing, (b):  $d+is$  pairing. (c,d): Total free energy (c) and the current-phase relation (d) in the  $d+s$  case (solid lines) and  $d+is$  case (dashed lines).

The case of  $d+is$  pairing is more complicated. In fact, first order coupling between the conventional superconductor and the  $s$ -wave component leads to a term in free energy  $-F_1 \cos(\varphi_{\text{conv}} - \varphi_s)$ , where  $\varphi_{\text{conv}}$  and  $\varphi_s$  are the phases of the conventional superconductor and of the  $s$ -wave component in YBCO and  $F_1 > 0$ . On the other hand, the second order term is the same as in the  $d+s$  scenario. Therefore, since  $\varphi = \varphi_{\text{conv}} - \varphi_d$  where  $\varphi_d$  is the phase of the  $d$ -wave component in YBCO, and since  $\varphi_s - \varphi_d = \pi/2$  in the  $d+is$  scenario, the junction free energy can be written

$$F(\varphi) = -F_1 \cos(\varphi - \varphi_{\min}) - F_2 \cos 2(\varphi - \varphi_{\min}), \quad (18)$$

where  $\varphi_{\min} = \pi/2$  is the equilibrium phase difference and  $F_1, F_2 > 0$ , see Fig. 7. In the experiment it is a delicate issue to determine the absolute value of  $\varphi_{\min}$ . Usually  $\varphi_{\min}$  is set equal to zero in the free energy minimum and with such conventions the two cases Eqs. 17,18 lead to a different relative sign of  $I_1$  and  $I_2$  for the  $d+s$  and  $d+is$  scenarios, respectively.

**2.3. FACETED JUNCTIONS.** In situations when the first harmonic  $I_1$  vanishes by symmetry (i.e. for asymmetric  $45^\circ$  grain boundary junctions or for  $c$ -axis tunneling between an  $s$ -wave and a  $d$ -wave superconductor), small local deviations from ideal geometry lead to a finite local coupling  $\delta I_1$  across the junction. In such cases the junction can be viewed as a parallel series of Josephson junctions with local critical current whose magnitude and sign fluctuate along the interface. It is customary to call the junctions with a positive (negative)  $\delta I_1$  as 0 and  $\pi$  junctions, respectively. Let us note in passing that very recently it has become possible to prepare samples with a prescribed pattern of 0 and  $\pi$  junctions, making use of the so-called zigzag junctions [32].

An example of a series of 0 and  $\pi$  junctions is shown in Fig. 8, where the geometry of an asymmetric  $45^\circ$  grain boundary between two twinned YBCO samples is shown. Twinning in the grain with  $\theta_1 = 0^\circ$  is not shown explicitly, since it is irrelevant for our argument. Another often considered source of deviations from ideal interface geometry is associated with the experimentally well documented meandering of interface [12].

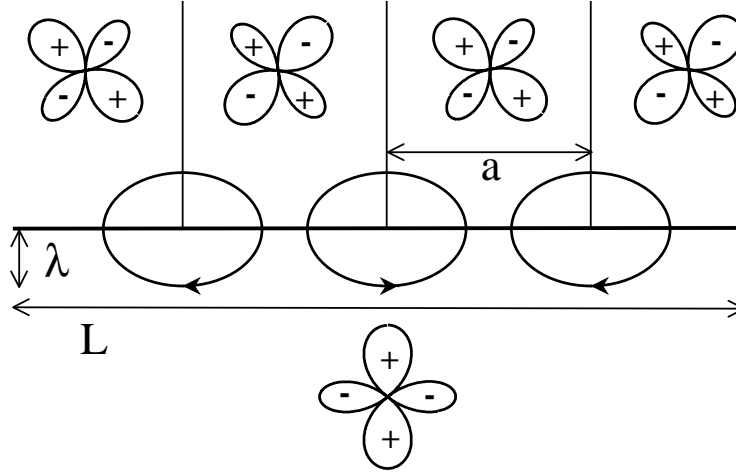


Figure 8: Schematic drawing of an asymmetric  $45^\circ$  grain boundary junction between twinned YBCO superconducting grains. In the upper grain the sign of the dominant lobe of the order parameter changes between the neighboring twins, leading to a sequence of 0 and  $\pi$  junctions. Also shown are the spontaneously generated currents along the interface.

If the average interface geometry is close to ideal, the number of 0 and  $\pi$  junctions is roughly the same. As noted first by Millis [14] (for an alternative formulation making use of the sine-Gordon equation, see e.g. [12, 33]), this does not imply a vanishing Josephson coupling across the interface. The general idea is as follows: let the average phase difference across the junction is  $\varphi$ . The phase difference along the interface is modulated from this value towards 0 and  $\pi$  in the 0 and  $\pi$  junction regions, respectively, by an amount  $\sim \chi$ . This leads to spontaneously generated currents along the interface which are schematically depicted in Fig. 8. In this way, the junction gains Josephson energy  $\propto \chi$ , whereas a Meissner energy of only  $\propto \chi^2$  is lost. The total energy gain is maximal for  $\varphi = \pm\pi/2$  and this explains qualitatively the development of a second harmonic in such junctions.

In what follows, let us discuss the faceted scenario in more detail. For definiteness, we

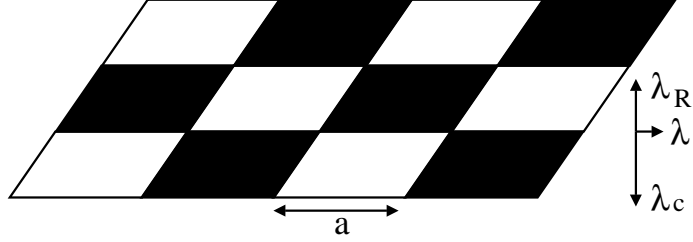


Figure 9: Schematic drawing of a  $c$ -axis junction between an  $s$ -wave superconductor and a twinned YBCO sample. The black and white regions (of typical size  $a$ ) correspond to 0 and  $\pi$  junctions, respectively. Also shown are the penetration depths in the  $s$ -wave superconductor ( $\lambda_R$ ) and in YBCO ( $\lambda, \lambda_c$ ).

consider the case of a  $c$ -axis junction between an  $s$ -wave superconductor and a twinned YBCO sample, see Fig. 9. For the sake of simplicity, we model the randomly twinned structure by a checkerboard distribution of 0 and  $\pi$  junctions with a periodic distribution of the local critical current density  $j_c(\mathbf{x}) = j_0 g(\mathbf{x})$ , where  $g(\mathbf{x}) = \sin(\pi x/a) \sin(\pi y/a)$  and for  $a$  we take the typical size of the twins. Here we have assumed a coordinate system such that the interface lies in the  $xy$  plane. According to [14], a spontaneous magnetic field is generated, which we now find by minimization of the total junction energy as a function of the phase difference  $\varphi$  across the junction. The symmetry of the problem dictates that the magnetic field reads

$$\begin{aligned} B_x &= \sum'_n B_n \exp(-K_n |z|) \sin(n\pi x/a) \cos(n\pi y/a), \\ B_y &= -\sum'_n B_n \exp(-K_n |z|) \cos(n\pi x/a) \sin(n\pi y/a), \\ B_z &= 0, \end{aligned} \tag{19}$$

where the prime restricts the summation to odd values of  $n$ . Note that  $\nabla \cdot \mathbf{B} = 0$ , as it should be. For  $z > 0$ , i.e. in the conventional superconductor, the  $\mathbf{B}$  field satisfies the equation  $(\nabla^2 - \lambda_R^{-2})\mathbf{B} = 0$  if  $K_n^2 = \lambda_R^{-2} [1 + 2n^2 (\pi \lambda_R/a)^2]$ . On the other hand, in the anisotropic cuprates,  $\mathbf{B} = (B_x, B_y, 0)$  is governed by  $B_{x,y} = [\lambda_c^2 (\partial_x^2 + \partial_y^2) + \lambda^2 \partial_z^2] B_{x,y}$  and therefore for  $z < 0$  we have to take  $K_n^2 = \lambda^{-2} [1 + 2n^2 (\pi \lambda_c/a)^2]$ . From Eq. 19, the distribution of Meissner screening currents can be calculated using  $\nabla \times \mathbf{B} = \mu_0 \mathbf{j}$ . The total junction energy per unit area corresponding to the magnetic field described by Eq. 19 is

$$E_\square = \frac{1}{4\mu_0} \sum'_n B_n^2 \lambda_n - \frac{\Phi_0 j_0}{2\pi S} \int dS g(\mathbf{x}) \cos \theta(\mathbf{x}), \tag{20}$$

where  $S$  is the junction area and

$$\lambda_n = \lambda_R \sqrt{1 + 2n^2 (\pi \lambda_R/a)^2} + \lambda \sqrt{1 + 2n^2 (\pi \lambda_c/a)^2}.$$

The local phase difference across the junction  $\theta(\mathbf{x})$  can be determined from the Josephson equations

$$\begin{aligned}\frac{\partial\theta}{\partial x} &= \frac{2\pi\mu_0}{\Phi_0} \left[ \lambda^2 j_x(z=0_-) - \lambda_R^2 j_x(z=0_+) \right] = \frac{2\pi}{\Phi_0} \sum'_n B_n \lambda_n \cos \frac{n\pi x}{a} \sin \frac{n\pi y}{a}, \\ \frac{\partial\theta}{\partial y} &= \frac{2\pi\mu_0}{\Phi_0} \left[ \lambda^2 j_y(z=0_-) - \lambda_R^2 j_y(z=0_+) \right] = \frac{2\pi}{\Phi_0} \sum'_n B_n \lambda_n \sin \frac{n\pi x}{a} \cos \frac{n\pi y}{a}.\end{aligned}\quad (21)$$

These equations are solved by  $\theta(\mathbf{x}) = \varphi + \chi(\mathbf{x})$ , where  $\varphi$  is the average phase difference and

$$\chi(\mathbf{x}) = \frac{2a}{\Phi_0} \sum'_n \frac{B_n \lambda_n}{n} \sin \frac{n\pi x}{a} \sin \frac{n\pi y}{a} \quad (22)$$

is the spontaneously generated modulation of  $\theta(\mathbf{x})$ .

The Fourier components  $B_n$  have to be determined by minimization of the energy Eq. 20. To this end let us assume now that  $|\chi| \ll 1$ , which assumption will be justified at the end of the calculation. The second term in Eq. 20 simplifies in this case to  $(2\mu_0)^{-1} B_1 B_{\text{eff}} \lambda_1 \sin \varphi$ , where  $B_{\text{eff}} = (2\pi)^{-1} \mu_0 j_0 a$ . Note that Fourier components  $B_n$  with  $n \geq 3$  raise the energy and therefore vanish. This means that the junction energy is at the end a function only of  $B_1$ ,  $E_\square = (\lambda_1/4\mu_0) \left[ (B_1 + B_{\text{eff}} \sin \varphi)^2 - B_{\text{eff}}^2 \sin^2 \varphi \right]$ . The minimum is reached for  $B_1 = -B_{\text{eff}} \sin \varphi$ . The minimized value of the junction energy density and the resulting current-phase relation read

$$\begin{aligned}E_\square(\varphi) &= -\frac{B_{\text{eff}}^2 \lambda_1}{4\mu_0} \sin^2 \varphi, \\ j(\varphi) &= -\frac{\pi B_{\text{eff}}^2 \lambda_1}{2\mu_0 \Phi_0} \sin 2\varphi.\end{aligned}\quad (23)$$

Note that  $j \propto j_0^2 \propto \mathcal{D}^2$ . Therefore the second harmonic scales with the barrier transparency in the same way both within the flat (for  $T \gg \mathcal{D}\Delta$ ) and the faceted scenario. Finally, let us point out that the result Eq. 23 is valid only for  $|\chi| \ll 1$ , or equivalently for

$$B_{\text{eff}} \ll \frac{\Phi_0}{2a\lambda_1}. \quad (24)$$

**2.4. THE JOSEPHSON PRODUCT.** According to standard theory (for homogeneous featureless barriers), the Josephson product  $I_1 R_N$  (where  $R_N$  is the junction resistance in the normal state) is independent of the junction area and of the barrier transparency, thus giving an intrinsic information about the superconducting banks. The measured Josephson product of cuprate grain boundary junctions [7] can be well described by  $I_1 R_N = \alpha^2 (\pi/4) (\Delta/e) \cos 2\theta$ , where  $\Delta$  is the maximal superconducting gap. The angular dependence of  $I_1 R_N$  is fully consistent (apart from the  $\theta$ -independent renormalization factor  $\alpha^2 \sim 10^{-1}$ ) with the BCS prediction Eq. 4 for rough junctions between  $d$ -wave superconductors. This means that

$$(I_c + I_s) R_N = \alpha^2 (\pi/2) (\Delta/e), \quad (25)$$



much smaller than the theoretical prediction Eq. 3 for  $I_c R_N$ . Note that the interpretation of a small factor  $\alpha^2$  as a result of a nearly complete cancellation of  $I_c$  and  $I_s$  is not plausible, since the cancellation would have to occur for all misorientation angles, whereas the physical origin of the  $I_c$  and  $I_s$  terms is quite different.

It is worth pointing out that Eq. 25 applies (with the same  $\alpha^2 \sim 10^{-1}$ ) also for the break junctions (in which the misorientation angle  $\theta = 0$ ) [34]. Moreover, in [34] it has been shown that  $\Delta$  is not depressed in the junction region, thus explicitly demonstrating the breakdown of the BCS prediction for  $I_1 R_N$  in the cuprates.

There exists no generally accepted explanation of the small renormalization factor  $\alpha^2$ . One of the reasons is that the microstructure of Josephson junctions is typically quite complicated. In fact, it is well known that small angle grain boundaries can be modelled by a sequence of edge dislocations, while at larger misorientation angles the dislocation cores start to overlap and no universal picture applies to the structure of the grain boundary. For large-angle grain boundaries, Halbritter has proposed [35] that the junction can be thought of as a nearly impenetrable barrier with randomly placed highly conductive channels across it. If due to strong Coulomb repulsion only the normal current (and no supercurrent) is supported by these channels, the small value of  $I_1 R_N$  follows quite naturally.

On the other hand, we have argued [36] that the smallness of the Josephson product does not follow from the particular properties of the barrier, but is rather an intrinsic property of the cuprates. Such a point of view has been first advocated in [37]. However, that paper did not consider alternative more conventional explanations. In order to support our point of view, in [36] we have discussed the Josephson product for intrinsic Josephson junctions in the  $c$ -axis direction. Such junctions can be viewed as an analogue of  $ab$ -plane break junctions (since the misorientation angle vanishes for both), but are preferable because of simpler geometry of the interface. Moreover, zero energy surface bound states which may develop at  $ab$ -plane surfaces because of the  $d$ -wave symmetry of the pairing state [13] do not form in the  $c$ -axis direction, simplifying the analysis of intrinsic Josephson junctions. By an analysis of the experimental data [38], we came to the conclusion that the experimental Josephson product is reduced with respect to theoretical predictions. Thus we have shown that although the barriers in grain boundaries and in intrinsic Josephson junctions are of very different nature, both types of junctions exhibit a suppressed Josephson product. Therefore we concluded that this suppression is not due to specific barrier properties as suggested in [35], but rather due to some intrinsic property of the high- $T_c$  superconductors.

### 3. EXPERIMENT

As shown in the previous Section, theory predicts anomalous behavior of the Josephson current in the cuprates as a function of the phase difference  $\varphi$  and temperature. One of the most striking predicted phenomena is a non-monotonic temperature dependence of the Josephson critical current, forced by the negative contribution of anomalous Andreev states. However, this has not been observed by standard means in spite of enormous efforts of many groups. The main obstacle seems to originate from the interface roughness which

leads to a suppression of the anomalous Andreev states [39, 40]. Even the most promising type of Josephson junctions, grain boundary junctions, contain defects on a characteristic scale of  $1\text{ }\mu\text{m}$  (Fig. 2 of [12]) coming from defects in the bicrystal substrate, see Fig. 10. A similar problem is relevant also in  $c$ -axis Josephson junctions, where a large second harmonic of the Josephson current is expected. In that case, in order to avoid tunneling in the  $ab$  plane direction and to achieve a high transparency of the interface, atomically flat surfaces are required.

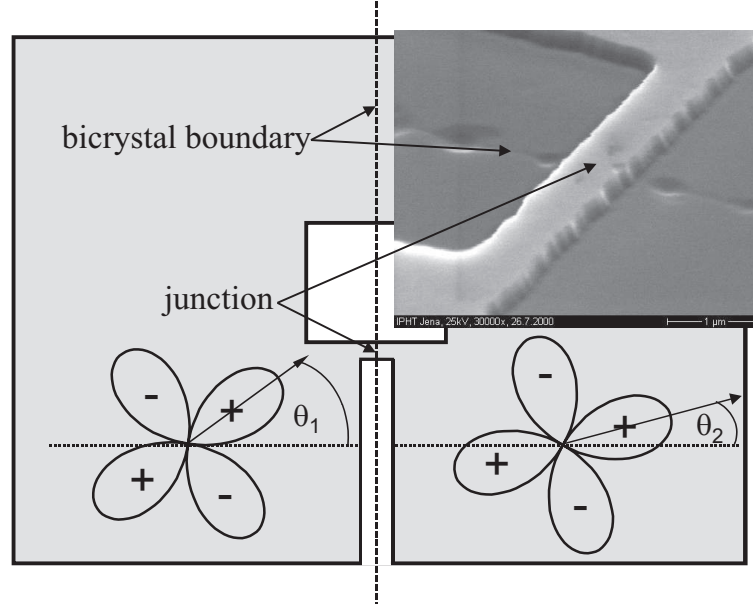


Figure 10: Schematic picture of the RF SQUID (taken from [4]). The YBCO thin film occupies the gray area. The inset shows an electron microscope image of the narrow grain boundary Josephson junction.

Thus, in order to observe the predicted anomalies, one should avoid the structural defects at the interface. Following this strategy the  $c$ -axis Josephson junctions were prepared in situ by covering YBCO by thick Au layer preventing the degradation of the YBCO surface during processing. On the other hand, we have chosen the position of the grain boundary junctions in such a way that they were placed between the defects of the substrate shown in Fig. 10. Therefore we were forced to reduce the size of the junction below  $1\text{ }\mu\text{m}$ . However, for submicron  $45^\circ$  junctions where the anomalies should be most pronounced, the Josephson coupling energy  $E_J$  is comparable with  $T$  in the temperature range of interest. This leads to large phase fluctuations and consequently to a suppression of the Josephson current. At first sight it seems that the Josephson current of submicron  $45^\circ$  junctions cannot be measured. But this is not so.

**3.1. EXPERIMENTAL METHOD.** Phase fluctuations can be suppressed by connecting the Josephson junction into a ring (rf SQUID), since in that geometry the phase difference across the junction is controlled by the large phase stiffness of the superconducting ring. This technique therefore offers a unique possibility to study Josephson junctions at temperatures  $T$  much higher than the junction energy. In addition, one can change the

phase difference  $\varphi$  on the Josephson junction by applying external magnetic flux  $\Phi_{dc}$  to the ring

$$\varphi = \varphi_{dc} - \frac{2\pi L_s}{\Phi_0} I(\varphi), \quad (26)$$

where  $\varphi_{dc} = 2\pi\Phi_{dc}/\Phi_0$ ,  $L_s$  is the inductance of the rf SQUID, and  $I(\varphi)$  is the Josephson current. We have used the modified Rifkin-Deaver method [41, 42] to restore the current-phase dependence  $I(\varphi)$ . The method is simple: The rf SQUID is inductively coupled to a high-quality parallel resonance circuit driven at its resonant frequency  $\omega_0$ . The angular phase shift  $\alpha$  between the rf driving current  $I_{rf}$  and the voltage across the circuit is measured by a rf lock-in voltmeter as a function of the external magnetic flux. The flux is set by a dc current  $I_{dc}$  through the coil of the resonant circuit with inductance  $L_T$ . Thus the total external magnetic flux can be expressed as  $\varphi_e = \varphi_{dc} + \varphi_{rf}$ , where  $\varphi_{dc} = 2\pi M I_{dc}/\Phi_0$  and  $\varphi_{rf} = 2\pi M I_{rf}/\Phi_0$  and  $M$  is the mutual inductance between the rf SQUID and the resonant circuit. The rf SQUID and the resonant circuit are characterized by quality factors  $q = \omega_0 L_s/R$  and  $Q = R_T/\omega_0 L_T$ , respectively. The analysis of such a system can be considerably simplified in the adiabatic ( $q \ll 1$ ,  $Q \gg 1$ ), small signal regime ( $\varphi_{rf} \ll 1 + (2\pi L_s/\Phi_0)dI(\varphi)/d\varphi$ ), when the rf SQUID follows adiabatically the signal from the resonant circuit and the internal flux can be expressed by Eq. 26.  $I(\varphi_{dc})$  is calculated from the experimental  $\alpha(\varphi_{dc})$  data using

$$I(\varphi_{dc}) = \frac{L_T I_0^2}{2\pi Q \Phi_0} \int_0^{\varphi_{dc}} \tan \alpha(\varphi_{dc}) d\varphi_{dc}, \quad (27)$$

where  $I_0$  is the period of  $\alpha(I_{dc})$  (i.e.  $M I_0 = \Phi_0$ ) and the quality factor  $Q$  is measured independently from the width of the resonance curve of the parallel resonant circuit. Using Eqs. 26,27  $I(\varphi)$  can be restored. This method, being differential with respect to  $\varphi$ , provides a high sensitivity of the current phase measurement.

Let us emphasize that the critical current determined by this method does not depend on the inductance of the rf SQUID. In fact, one can easily show that  $I_c = I(\varphi_{dc}^0)$ , where  $\tan \alpha(\varphi_{dc}^0) = 0$  can be determined from experimental data by requiring  $\int_0^\pi \tan \alpha(\varphi_{dc}) d\varphi_{dc} = 0$ . The last condition comes from the periodicity of  $I(\varphi)$  and enables a subtraction of a constant phase shift coming from electronics and cables. Since the only sample characteristics entering Eq. 27 is  $I(\varphi)$ , the measurement system can be calibrated using samples with known critical current and  $I(\varphi)$ . We have usually carried out the calibration making use of Nb rf SQUIDS. Typical values of the quantities used in our experimental setup are:  $L_s = 80$  pH,  $L_t = 0.27$   $\mu$ H,  $Q = 155$ . Critical currents measured by the present method and by standard transport measurements were in good coincidence. As already explained,  $I(\varphi)$  is measurable even if the thermal energy exceeds the Josephson coupling energy. In fact, critical currents down to 50 nA were recently detected at  $T = 4.2$  K [4] using cooled preamplifier placed near the parallel resonant circuit. All  $I(\varphi)$  measurements presented in this paper have been performed in a gas-flow cryostat with a five-layer magnetic shielding in the temperature range  $1.6 \leq T < 90$  K.

**3.2. GRAIN BOUNDARY JOSEPHSON JUNCTIONS.** The rf SQUIDS were prepared at IPHT Jena by laser deposition of YBCO thin films of thickness 100 nm on bicrystal substrates. They were patterned in the shape of a square washer  $3500 \mu\text{m} \times 3500 \mu\text{m}$  with a

hole  $50\text{ }\mu\text{m}\times 50\text{ }\mu\text{m}$  by electron beam lithography (see Fig. 10). The estimated Josephson penetration depth  $\lambda_J$  is much smaller than the width of the wide junction,  $w_l = 1725\text{ }\mu\text{m}$ , and larger than the width of the narrow junction,  $w_s = 1\text{ }\mu\text{m}$  and  $w_s = 0.7\text{ }\mu\text{m}$  for asymmetric and symmetric  $45^\circ$  junctions, respectively. Thus the behavior of the rf SQUID is dictated by the narrow junction only. For symmetric  $45^\circ$  junctions the submicron bridge was formed at a position between the defects of the substrate which are visible in Fig. 10. The experimental results are shown in Fig. 11. Local minima appear at low temperatures on the  $\alpha(\varphi_{dc})$  curve close to  $\varphi_{dc} = 2\pi n$  where  $n$  is integer. The existence of the local minima dictates

$$\left. \frac{d^3 I(\varphi)}{d\varphi^3} \right|_{\varphi=2\pi n} > 0. \quad (28)$$

Note that neither the conventional tunneling theory nor the I and II theories by Kulik and Omelyanchuk predict such local minima on the derivatives of CPR [1].

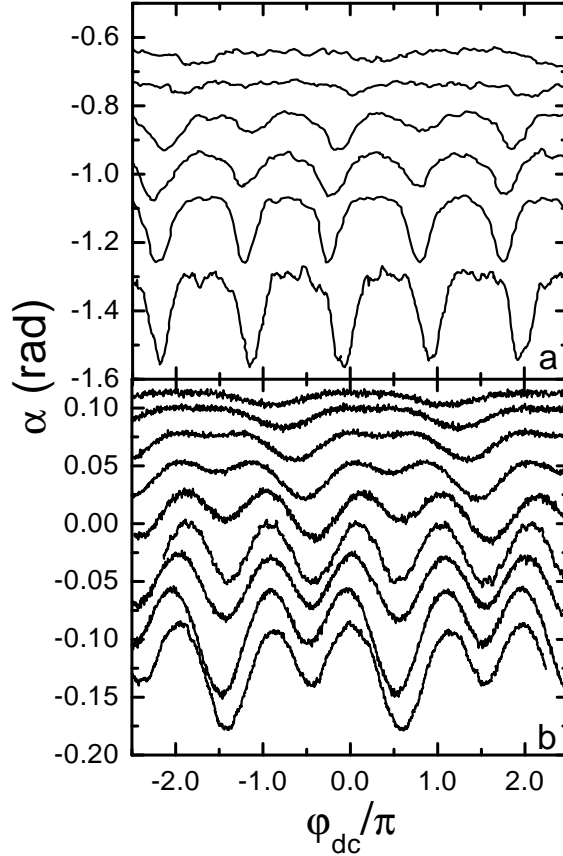


Figure 11: The phase angle  $\alpha$  as a function of  $\varphi_{dc}$  measured at different temperatures. (a) Asymmetric  $45^\circ$  grain boundary [3]. Top to bottom curves correspond to  $T = 40, 30, 20, 15, 10$ , and  $4.2$  K, respectively. (b) Symmetric  $45^\circ$  grain boundary [4]. Top to bottom curves correspond to  $T = 35, 30, 25, 20, 15, 11, 10, 5$ , and  $1.6$  K, respectively.

To demonstrate that the anomalous behavior of the Josephson current is a peculiarity of  $45^\circ$  junctions we have measured  $I(\varphi)$  of symmetric YBCO grain boundary junctions

with misorientations  $\theta = 24^\circ$  and  $36^\circ$ . The results of this study are shown in Fig. 2. We have found that the critical current decreases exponentially with the misorientation angle  $\theta$ ,  $\exp(-\theta/\theta_0)$  with  $\theta = 5.6^\circ$ , in good agreement with [43]. Moreover, both for  $\theta = 24^\circ$  and  $36^\circ$ , no considerable deviation from sinusoidal dependence of  $I(\varphi)$  was observed, implying tunneling as the dominant transport mechanism.

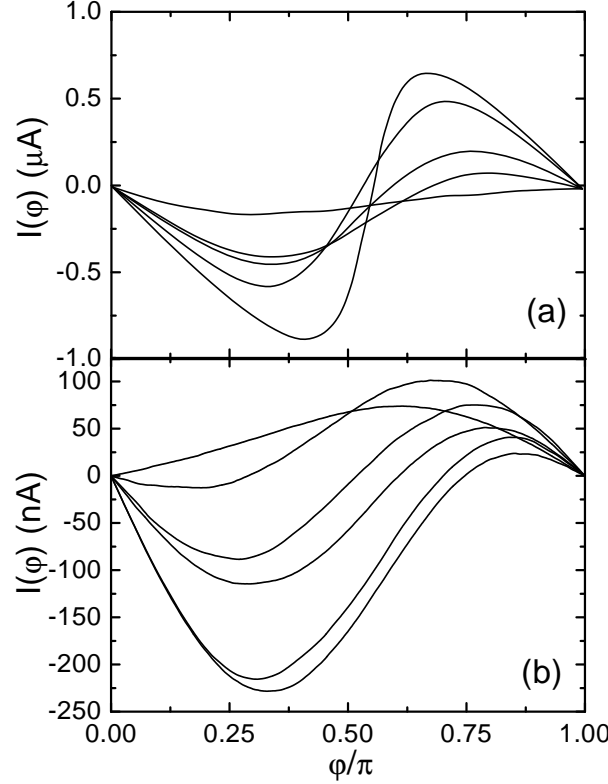


Figure 12: Current-phase relation for asymmetric (a) and symmetric (b)  $45^\circ$  grain boundary junctions (taken from [6]). (a) Top to bottom curves at  $\varphi = 0.75\pi$ :  $T = 4.2, 10, 15, 20$ , and  $30$  K. (b) Bottom to top curves at  $\varphi = 0.375\pi$ :  $T = 1.6, 5, 10, 11, 15$ , and  $25$  K.

Let us return to the case of  $45^\circ$  junctions now. Theory predicts that the first harmonic should be suppressed for such junctions. If we in addition take into account that the barrier transmission is low, we can model  $I(\varphi)$  of such junctions by neglecting terms of higher orders ( $n > 2$ ) in Eq. 1. Therefore the condition (28) for the existence of the local minima at  $\varphi_{dc} = 2\pi n$  dictates  $I_2/I_1 < -1/8$ . Thus we conclude that the  $45^\circ$  junctions exhibit anomalously large second harmonic of the Josephson current which has opposite sign in comparison with  $I_1$ . The current-phase relations calculated from the experimental data in Fig. 11 are shown in Fig. 12. Note the anomalous form of  $I(\varphi)$  at low temperatures. The temperature dependence of the first two harmonics  $I_1$  and  $I_2$ , determined from a Fourier analysis of  $I(\varphi)$ , is shown in Fig. 13. For both asymmetric and symmetric  $45^\circ$  junctions the second harmonic monotonically increases as the temperature decreases. The first harmonic is more or less constant for asymmetric junctions whereas for symmetric  $45^\circ$  junctions the first harmonic starts to exhibit a downturn below  $20$  K. The most striking result is that for  $T=12$  K,  $I_1$  changes sign. In the same temperature region

where  $I_1$  starts to exhibit a downturn, the absolute value of  $I_2$  rises from a negligible value at high temperatures to values comparable to  $I_1$  at low temperature. This experimental fact suggests a common origin of both phenomena. Similar effects were theoretically predicted for Josephson junctions between  $d$ -wave superconductors (Section 2) and our experiments can be therefore regarded as an independent experimental test of the  $d$ -wave symmetry of pairing in YBCO.

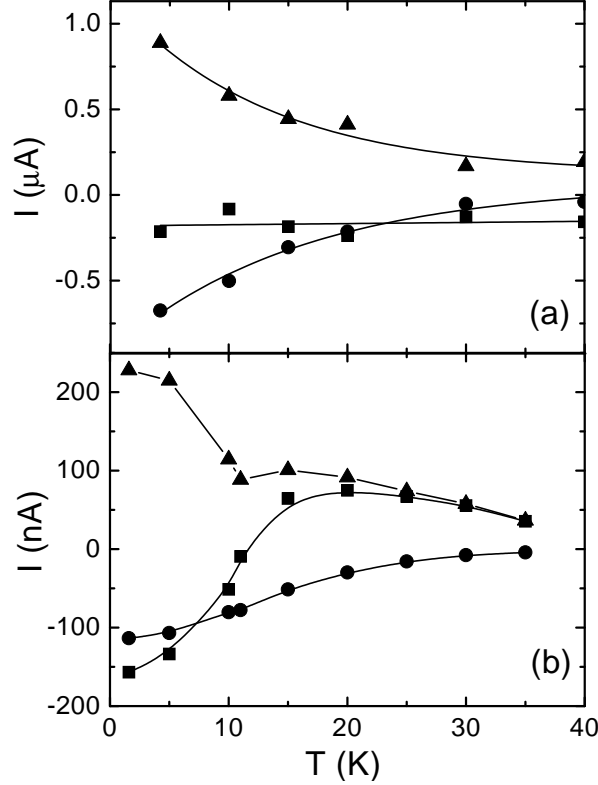


Figure 13: Critical current  $I_c$  (triangles) and the first two harmonics  $I_1$  (squares) and  $I_2$  (circles) as a function of temperature for asymmetric (a) and symmetric (b) grain boundary  $45^\circ$  junctions (taken from [6]). The lines are guides to the eye.

**3.2.  $c$ -AXIS JOSEPHSON JUNCTIONS.** The  $c$ -axis Josephson junctions were fabricated and characterized jointly by the IRE Moscow and Chalmers groups following [44]. Epitaxial (001)-oriented YBCO thin films with thickness 150 nm were obtained by laser deposition on (100)  $\text{LaAlO}_3$  and (100)  $\text{SrTiO}_3$  substrates and *in situ* covered by a  $8 \div 20$  nm thick Au layer, thus preventing the degradation of the YBCO surface during processing. Afterwards, 200 nm thick Nb counterelectrodes were deposited by DC-magnetron sputtering. Junctions with dimensions  $10 \times 10 \mu\text{m}^2$  were formed by photolithography and low energy ion milling techniques. The interface resistance per unit area  $R_\square = R_N S$  (where  $R_N$  is the normal state resistance and  $S$  is the junction area) was  $R_\square = 10^{-5} \div 10^{-6} \Omega \cdot \text{cm}^2$ . Details of the junction fabrication were reported elsewhere [44].

Surface quality of the YBCO films is very important when current transport in the  $c$ -direction is investigated. High-resolution atomic force microscopy reveals a smooth surface

consisting of approximately 100 nm long islands with vertical peak-to-valley distance of  $3 \div 4$  nm [5]. We can exclude that substantial  $ab$ -plane tunnel currents flow between YBCO and Nb at the boundaries of these islands. In fact, theory predicts formation of midgap states at the surface of semi-infinite  $\text{CuO}_2$  planes [13, 45]. Therefore zero bias conductance peaks should be expected in the  $I$ - $V$  characteristics at temperatures larger than the critical temperature of Nb, if the contribution of  $ab$ -plane tunneling was nonnegligible. However, no such peaks have been observed for all fabricated Nb/Au/YBCO junctions. Moreover, from the size of the islands and from the vertical peak-to-valley distance we estimate that the area across which  $ab$ -plane tunneling might take place is only  $\approx 6\%$  of the total junction area. However, since the interface resistances per square are of the same order of magnitude [27] for both, the  $c$ -axis and  $ab$ -plane junctions, we conclude that  $ab$ -plane tunneling from YBCO, if present, is negligibly small.

More than 20 junctions were characterized by transport measurements. At small voltages typical  $I$ - $V$  curves can be described by the resistively shunted junction model with a small capacitance [1]. Typical critical current densities were  $j_c = 1 \div 12$  A/cm<sup>2</sup> and  $j_c R_\square = 10 \div 90$   $\mu\text{V}$ . The differential resistance *vs.* voltage dependence  $R_d(V)$  exhibits a gap-like structure at  $V \approx 1.2$  mV. This structure has a BCS-like temperature dependence and disappears at  $T_{cR} \approx 9.1$  K, therefore we ascribe it to the superconducting energy gap of Nb.

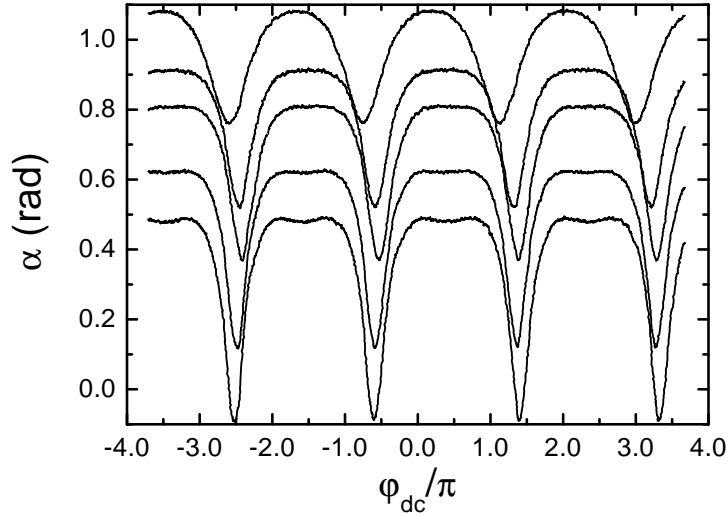


Figure 14: Phase shift  $\alpha$  as a function of  $\varphi_{dc}$  for a  $c$ -axis junction at  $T=1.7, 2.5, 3.5, 4.2$ , and 6.0 K (from bottom to top). Taken from [5].

The current phase relation of the  $c$ -axis Josephson junctions was measured by closing the Nb/Au/(001)YBCO heterostructure into a superconducting ring with the same geometry as for  $45^\circ$  grain boundary junctions. The experimental results are shown in Figs. 14,15. When compared with  $45^\circ$  junctions, the second harmonic of the Josephson current was considerably smaller but still anomalously large, leading to local minima of  $\alpha(\varphi_{dc})$ . As follows from the analysis in Section 2.2, the opposite signs of the first and second harmonics of the Josephson current provide direct evidence that in our YBCO samples, pairing with a macroscopic  $d + s$  symmetry is realized. The large first harmonic

has to be due to an uncompensated  $s$ -wave component whose origin is discussed in detail in the next Section.

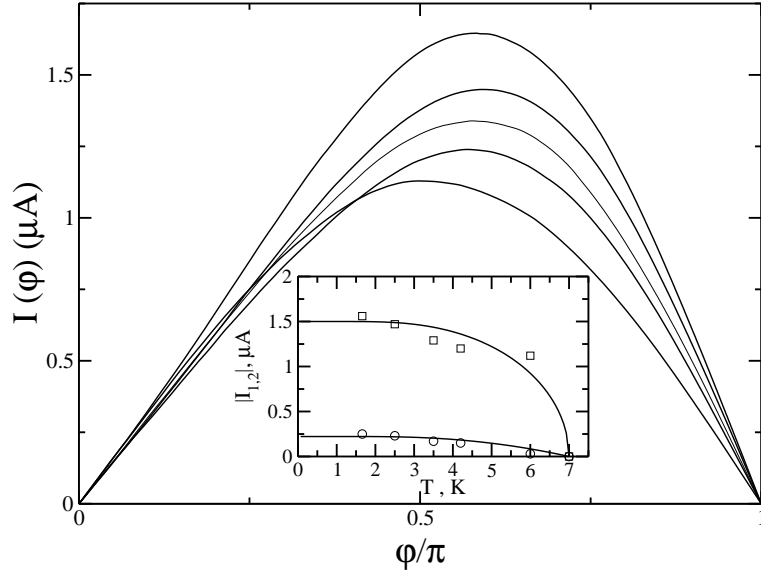


Figure 15: The current-phase relation  $I(\varphi)$  of the  $c$ -axis junction from Fig. 14 at  $T=1.7, 2.5, 3.5, 4.2$ , and  $6.0$  K (from top to bottom). Inset: Temperature dependence of  $I_1$  (squares) and  $|I_2|$  (circles). Solid lines are fits to Eqs. (31,32) using  $\Delta_R(T) = \Delta_R(0) \tanh[\Delta_R(T)T_{cR}/\Delta_R(0)T]$ . Taken from [5].

## 4. DISCUSSION

**4.1. GRAIN BOUNDARY JUNCTIONS. *Asymmetric 45° junctions.*** The large second harmonic observed in [3] confirms the naive expectations based on the symmetry of the pairing state in the cuprates. However, at the time of writing the paper [3], we were not able to explain the details of the shape of the current-phase relation. In particular, we could not find any mechanism leading to a current-phase relation which was steep in the minima and flat in the maxima of energy. For instance the Kulik-Omelyanchuk theory [1] leads to an exactly opposite picture of jumps in  $I(\varphi)$ , which occur in the maxima of energy (at  $\varphi = \pm\pi$ ). This is a consequence of the fact that for  $\varphi = \pm\pi$  two locally stable branches of the junction energy cross, one centered around  $\varphi = 0$  and another one around  $\varphi = \pm 2\pi$ . We believe that in the present work we have found one physically plausible scenario for how the pattern of jumps of  $I(\varphi)$  observed in [3] can be explained. In fact, Fig. 6 shows that behavior qualitatively similar to the results of [3] obtains if the Meissner energy dominates the junction energy Eq. 11. A more detailed investigation of this idea is under way. A preliminary analysis indicates that in order to be applicable to [3], also the effect of a spatially fluctuating barrier similar to that discussed at the end of Section 4.2 needs to be taken into account.

Although consistent with naive expectations, under closer inspection, the experimentally found large value of the second harmonic remains mysterious:



In the flat scenario, the second harmonic is given by Eq. 12. On the other hand, by combining Eqs. 4,25 we estimate that the first harmonic  $j_1 R_\square \approx \pi \alpha^2 \delta \Delta / e$ , where  $\delta$  is the deviation of the misorientation angle  $\theta$  from the nominal value of  $45^\circ$ . Taking a realistic value of such a deviation at least  $\delta \sim 10^{-2}$ , by comparing to Eq. 12 we find that the experimental value  $j_2/j_1 \sim 1$  can be explained, only if  $\vartheta_0 \sim 1$  (and therefore the tunneling has to be possible in a wide range of impact angles). In this estimate we have made use of the well established [7] value  $\mathcal{D} \sim 10^{-4}$  and we have taken  $\Delta/T \sim 10^2$  at helium temperatures. Note that in order to obtain  $j_2/j_1 \sim 1$  we had to assume that only the first harmonic is renormalized by  $\alpha^2 \sim 10^{-1}$ , while the second harmonic has to remain unrenormalized. This implies very peculiar microscopic physics.

Now let us consider the faceted scenario. As an order of magnitude estimate, we use the result Eq. 23 for the second harmonic. Unlike in the  $c$ -axis case, in the present case all penetration depths have to be set equal to the in-plane penetration depth of the cuprates  $\lambda \approx 0.15 \mu\text{m}$ . This yields  $j_2 = (8\pi\Phi_0)^{-1} \mu_0 j_0^2 a^2 \lambda_1$ , where  $\lambda_1 = 2\lambda\sqrt{1 + 2(\pi\lambda/a)^2}$ . For  $a$  we take the typical length scale of faceting,  $a \approx 0.1 \mu\text{m}$ , since the twin size is even smaller. This yields  $\lambda_1 \approx 2 \mu\text{m}$ . The only unknown in the expression for  $j_2$  is the local current density  $j_0$ . In what follows we determine  $j_0$  from  $j_0 = \sqrt{8\pi j_2 \Phi_0 / (\mu_0 a^2 \lambda_1)}$  where for  $j_2$  we take the experimental critical current density  $j_2 \sim 10^4 \text{ A/cm}^2$  [7], and we obtain a reasonable value  $j_0 \sim 10^6 \text{ A/cm}^2$ . Note that since  $B_{\text{eff}} = (2\pi)^{-1} \mu_0 j_0 a \approx 3 \times 10^{-4} \text{ T}$  and  $\Phi_0/(2a\lambda_1) \approx 5 \times 10^{-3} \text{ T}$ , the criterion Eq. 24 for the applicability of Eq. 23 is well satisfied. On the other hand, we estimate the first harmonic from  $j_1/j_0 \approx (a/L)^{1/2}$ , which is a random walk-type formula, indicating that  $j_1$  averages to zero in a sufficiently long junction. The experiment requires  $j_2 > j_1$ . This is possible only for sufficiently long junctions,  $L \sim 1 \text{ mm}$ , whereas in [3] much shorter junctions with  $L \sim 1 \mu\text{m}$  were studied. Therefore within the faceted scenario it is not possible to explain the large measured  $I_2/I_1$  ratio.

We conclude that both within the flat and faceted scenaria, the second harmonic measured in [3] appears to be anomalously large.

*Symmetric  $45^\circ$  junctions.* The anomalous temperature dependence of the first harmonic and the large second harmonic observed in this type of junctions [4] is qualitatively consistent with the theoretical prediction Eq. 15 and not with Eq. 16. The data seems to imply (as was the case for asymmetric junctions as well) that the impact angle dependence of the barrier transmission is weak.

In what follows we attempt a more quantitative discussion of the results found in [4]. According to Fig. 13 the first harmonic changes sign at a temperature  $T^* \approx 12 \text{ K}$ . This together with the estimate  $\Delta \approx 20 \text{ meV}$  [16] requires  $D(\pi/4)/D(0) \approx 0.1$ , i.e. the barrier, although presumably quite thin, can't be modelled by a delta function.

Now let us compare the relative magnitudes of the first and second harmonics. Theory predicts that for  $T > T^*$ , the maximal value of  $j_1$  is  $j_1^{\text{max}}/j_L \approx D(0)$ . On the other hand, from Eq. 15 it follows that at  $T = T^*$  the second harmonic  $|j_2(T^*)|/j_L \approx D(0)^3/24D(\pi/4)$ . Therefore according to theory  $|j_2(T^*)|/j_1^{\text{max}} \approx D(0)^2/24D(\pi/4) \approx D(0)/2$ , whereas from Fig. 13 we estimate  $|j_2(T^*)|/j_1^{\text{max}} \approx 1$ . Thus theory can describe the experimental results only if  $D(0) \sim 1$ .

However, in what follows we show that  $D(0) \ll 1$  and therefore the experimental sec-

ond harmonic is again too large when compared with simple minded theory. In fact, in order that higher-order harmonics are negligible [4] even at the lowest studied temperatures  $T_{\min} \approx 1.6$  K, we require that the typical mid-gap state energy  $\Delta\sqrt{D(\pi/4)/2} < 2T_{\min}$ , yielding  $D(\pi/4) < 4 \times 10^{-4}$ , and therefore  $D(0) \approx 10D(\pi/4) < 4 \times 10^{-3}$ . Moreover,  $D(0) \sim 10^{-3}$  seems to be consistent with the exponential decrease of  $j_c$  with the misorientation angle  $\theta$  [43].

In [6] we have proposed that the first harmonic might be suppressed by interface roughness according to Eq. 4. This would require a very small roughness parameter  $x \sim 10^{-3}$  and therefore the junction would have to be nearly completely rough. However, we have overlooked the fact that for such junctions it is hard to believe that the deviation  $\delta$  from the misorientation angle  $\theta = 45^\circ$  can be sufficiently small in order to keep the first term in Eq. 4 small.

In summary, the second harmonic of  $45^\circ$  grain boundary junctions seems to be too large to be explicable by conventional theory.

**4.2. *c*-AXIS JUNCTIONS.** Let us start by estimating the transparency of the barrier between YBCO and Nb from the normal-state resistance per unit area  $R_\square$ . According to the band-structure calculations (for a review, see [46]), the hole Fermi surface of YBCO is a slightly warped barrel with an approximately circular in-plane cross-section (to be called Fermi line) with radius  $k_F$ . In what follows, we represent the electron wavevector  $\mathbf{k}$  in cylindrical coordinates,  $\mathbf{k} = (k, \theta, k_z)$ . We estimate the uncertainty of the in-plane momentum as  $\delta k \approx 2\pi/l$ , where  $l$  is the characteristic size of the islands on the YBCO surface (fig.1). We evaluate  $R_\square$  making use of the Landauer formula and note that only tunneling from a shell around the Fermi line with width  $\delta k$  is kinematically allowed. The barrier transparency  $D(\theta)$  depends on the details of the *c*-axis charge dynamics in YBCO, with maxima in those directions  $\theta$ , in which the YBCO *c*-axis Fermi velocity  $w(\theta)$  is maximal. Since for  $\theta = \pi/4$  and symmetry equivalent directions  $w(\theta)$  is minimal [47], we expect that there will be 8 maxima of  $D(\theta)$  on the YBCO Fermi line where  $D(\theta) \approx D$ , which are situated at  $\theta = \theta_0$  and symmetry equivalent directions. The modulation of the function  $D(\theta)$  depends on the thickness of the barrier between YBCO and Nb [48]. We consider two limiting distributions of the barrier transparency  $D(\theta)$  along the YBCO Fermi line: (a) a featureless  $D(\theta) \approx D$  and (b) a strongly peaked  $D(\theta)$ , roughly corresponding to thin and thick barriers, respectively [48]. In the thick barrier limit the angular size of the maxima of  $D(\theta)$  can be estimated as  $\delta\theta \approx \delta k/k_F$ . With these assumptions we find

$$R_\square^{-1} = \frac{\langle D \rangle e}{\Phi_0} A, \quad (29)$$

where  $A$  measures the number of conduction channels and  $\langle \dots \rangle$  denotes an average over the junction area. In the thin and thick barrier limits, we find  $A \approx k_F \delta k / \pi$  and  $A \approx 2\delta k^2 / \pi$ , respectively. Taking  $l \approx 100$  nm and  $k_F \approx 0.6 \text{ \AA}^{-1}$  [49], the measured  $R_\square = 6 \times 10^{-5} \text{ } \Omega\text{cm}^2$  can be fitted with  $\langle D \rangle_{\text{thin}} \approx 1.7 \times 10^{-5}$  and  $\langle D \rangle_{\text{thick}} \approx 8.3 \times 10^{-4}$ .

Now we can turn to the discussion of  $I(\varphi)$ . Since we have observed no midgap surface states in the  $R_d(V)$  curves, we can neglect the surface roughness, and the Josephson

current can be calculated from [50]

$$I(\varphi) = \frac{2e}{\hbar} \sum_{k,\theta} k_B T \sum_{\omega} \frac{D \Delta_R \Delta_{\mathbf{k}} \sin \varphi}{2\Omega_R \Omega_{\mathbf{k}} + D [\omega^2 + \Omega_R \Omega_{\mathbf{k}} + \Delta_R \Delta_{\mathbf{k}} \cos \varphi]}, \quad (30)$$

where the sum over  $k, \theta$  is taken over the same regions with areas  $A$  as in Eq. (29),  $\Delta_R$  and  $\Delta_{\mathbf{k}}$  are the Nb and YBCO gaps, respectively, and  $\Omega_i = \sqrt{\omega^2 + \Delta_i^2}$  with  $i = R, \mathbf{k}$ . Keeping only terms up to second order in the (small) junction transparency  $D$ , the first and second harmonics of the Josephson current densities for an untwinned YBCO sample read

$$j_0(T) R_{\square} \approx \frac{\Delta_s}{\Delta_d^*} \frac{\Delta_R(T)}{e}, \quad (31)$$

$$j_2(T) R_{\square} \approx -\frac{\pi}{8} \frac{\langle D^2 \rangle}{\langle D \rangle} \frac{\Delta_R(T)}{e} \tanh \left( \frac{\Delta_R(T)}{2k_B T} \right), \quad (32)$$

where  $\Delta_d^* = \pi \Delta_d [2 \ln(3.56 \Delta_d / T_{cR})]^{-1}$  and  $\Delta_d^* = \Delta_d |\cos 2\theta_0|$  in the thin and thick barrier limits, respectively. In Eqs. (31,32) we have assumed that the angular variation of the YBCO gap can be described as  $\Delta(\theta) = \Delta_s + \Delta_d \cos 2\theta$ , where  $\Delta_d$  and  $\Delta_s$  are the  $d$ -wave and  $s$ -wave gaps. We have assumed that  $\Delta_d^*$  is larger than both,  $\Delta_R$  and  $\Delta_s$ . The factor  $\Delta_s / \Delta_d^*$  can be estimated from the measured  $j_0 R_{\square}$  products for Josephson junctions between untwinned YBCO single crystals and Pb counterelectrodes. For such junctions  $j_0(0) R_{\square} \approx 0.5 \div 1.6$  mV [27]. Using the Pb gap  $\Delta_R = 1.4$  meV in Eq. (31), we obtain  $\Delta_s / \Delta_d^* \approx 0.36 \div 1.1$ .

From the relative sign of  $I_1$  and  $I_2$  we know that the finite first harmonic has to be due to the macroscopic  $d + s$  symmetry of our YBCO sample. The simplest way how this can be realized is to assume that the numbers of the two types of twins are unequal. In fact, detailed structural studies show that this is the case for sufficiently thin YBCO films even if they are grown on the cubic substrate  $\text{SrTiO}_3$  [51]. If we denote the twin fractions as  $(1 + \delta)/2$  and  $(1 - \delta)/2$ , then the measured first harmonic of the CPR,  $j_1$ , is proportional to the deviation from equal population of twins,  $j_1 = \delta j_0$  [31]. Using  $\Delta_R = 1.2$  meV determined from the  $R_d(V)$  data and our estimate  $\Delta_s / \Delta_d^* \approx 0.36 \div 1.1$ , we find that the measured first harmonic  $j_1$  can be fitted with  $\delta \approx 0.07 \div 0.21$ , which is in qualitative agreement with [51], where  $\delta \approx 0.14$  for 1000 Å thick YBCO films has been observed.

Fitting the measured  $j_2 R_{\square}$  by Eq. (32),  $\langle D^2 \rangle / \langle D \rangle \approx 3.2 \times 10^{-2}$  was found, which is much larger than both  $\langle D \rangle_{\text{thin}}$  and  $\langle D \rangle_{\text{thick}}$ . Similarly as in the case of grain boundary junctions, this means that the experimental second harmonic is too large when compared with naive estimates. In what follows we discuss the possible causes of such behavior.

Let us start by considering the faceted scenario. From the known values of  $j_0 R_{\square}$  [27] and  $R_{\square}$  we estimate  $j_0 \approx 8 \div 27$  A/cm<sup>2</sup>. Taking for a typical twin size  $a \approx 10$  nm, the effective magnetic field from Section 2.3 is estimated as  $B_{\text{eff}} \approx (1.6 \div 5.4) \times 10^{-10}$  T. Moreover, since  $\lambda_R \approx 39$  nm,  $\lambda \approx 240$  nm, and  $\lambda_c \approx 3$  μm (as an upper bound, for the cuprates we take numbers which are valid for underdoped YBCO [52]), we find  $\lambda_1 \approx 320$  μm. Since this implies  $\Phi_0 / (2a\lambda_1) \approx 3 \times 10^{-4}$  T, the criterion Eq. 24 is seen to be well satisfied and therefore the second harmonic can be calculated from Eq. 23, yielding

$|j_2|R_\square \approx (3 \div 35) \times 10^{-11}$  V, orders of magnitude smaller than the experimental value  $|j_2|R_\square \approx 15$   $\mu$ V.

Thus we were led to look for alternative explanations of the large second harmonic. In [5] we came up with an explanation which assumed that the junction transparency  $D$  is a fluctuating function of the position  $\mathbf{r}$ . Adopting the WKB description of tunneling [48], we assumed that the local barrier transparency  $D(s(\mathbf{r})) = \exp(-s_0 - s(\mathbf{r}))$ , where  $s_0$  is the WKB tunneling exponent and  $s(\mathbf{r})$  its local deviation from the mean. Assuming a Gaussian distribution of  $s$  with a mean deviation  $\eta$ ,  $P(s) \propto \exp(-s^2/\eta^2)$ , we estimated the spatial averages as  $\langle D^n \rangle = \int_{-s_0}^{s_0} ds P(s) D^n(s)$ . In the thin barrier limit, the values  $\langle D^2 \rangle_{\text{thin}} = 8.6 \times 10^{-7}$  and  $\langle D \rangle_{\text{thin}} = 2.3 \times 10^{-5}$  required to fit the experiments correspond to an average WKB exponent  $s_0^{\text{thin}} \approx 15.5$  with  $\eta_{\text{thin}} \approx 4.3$ . In the thick barrier limit we obtain  $s_0^{\text{thick}} \approx 9.1$  and  $\eta_{\text{thick}} \approx 2.8$ .

**4.3. MICROSCOPIC IMPLICATIONS.** Very recently it has been pointed out by one of us [36] that the two apparently unrelated experimental facts, namely the suppressed Josephson product  $I_1 R_N$  and the enhanced ratio  $|I_2/I_1|$ , can be explained by a single assumption that in the cuprates some mechanism is operative which leads to a suppression of  $I_1$ , while leaving  $R_N$  and  $I_2$  intact. In what follows we describe one such mechanism which we believe to be the most promising one. Namely, we suggest that at low temperatures the superconducting state of the cuprates supports fluctuations of the superconducting phase. Such fluctuations presumably do not affect  $R_N$ , while they do influence the Josephson current. In simplest terms, if we denote the phases of the superconducting grains forming the junction as  $\phi_i$ , then the fluctuations renormalize the first and second harmonics by the factors  $\langle e^{i\phi_1} \rangle \langle e^{i\phi_2} \rangle$  and  $\langle e^{2i\phi_1} \rangle \langle e^{2i\phi_2} \rangle$ , respectively, where  $\langle \dots \rangle$  denotes a ground-state expectation value. Thus experiment requires that the fluctuations have to be of such type that  $|\langle e^{i\phi} \rangle| = \alpha \approx 0.3$  and  $|\langle e^{2i\phi} \rangle| \approx 1$ . Precisely this behavior is expected if the  $d$ -wave order parameter fluctuates towards  $s$ -wave pairing (which pairing is expected to be locally stable within several microscopic models of the cuprates).

An independent check of our picture is provided by measurements of the Josephson product for junctions between the cuprates and low- $T_c$  superconductors. In such a case, we predict that the Josephson product should be renormalized by a factor  $\alpha$  instead of  $\alpha^2$  for junctions between two cuprates. Junctions of this type have been studied extensively in the past. In particular,  $ab$ -plane junctions between YBCO and Pb exhibit Josephson products of  $0.2 \div 1.2$  mV [27]. On the other hand, Eq. 3 predicts  $I_c R_N \approx e^{-1} \Delta_{\text{Pb}} \ln(4\Delta_{\text{YBCO}}/\Delta_{\text{Pb}}) \approx 5.7$  mV in this case, if we assume a (100) YBCO surface and take  $\Delta_{\text{YBCO}} \approx 20$  meV and  $\Delta_{\text{Pb}} \approx 1.4$  meV. We interpret the large experimental scatter of  $I_c R_N$  as being due to varying  $ab$ -plane tunneling direction. Thus theory has to be compared with the largest experimental value, and the theoretical result has to be multiplied by a renormalization factor  $\alpha \approx 0.2$  in order to bring it in agreement with experiment. This value is in semiquantitative agreement with  $\alpha \approx 0.3$  which was determined from the Josephson product of grain boundary junctions. It is worth mentioning that the phase fluctuation picture also may be relevant for the experiment [5], where a large second harmonic has been found in a  $c$ -axis Josephson junction between YBCO and Nb.

## 5. CONCLUSIONS

In this paper we have tried to argue that the Josephson effect can provide nontrivial information not only about the symmetry of the pairing state in the cuprates, but also about the fluctuations of the superconducting order parameter. The latter are expected to be quite large especially in the underdoped region, where charge fluctuations should be suppressed. A preliminary analysis of the Josephson product and of the current-phase relation in grain boundary and *c*-axis junctions indicates [36] that the phase fluctuations of the superconducting order parameter are quite large and of a very special type, favoring local fluctuations from *d*-wave towards extended-*s* pairing.

Surprisingly, the potential of the Josephson effect as a test of the phase rigidity of the cuprates seems to have been missed in the past and therefore quite few studies have attempted quantitative analysis of the Josephson phenomena. Therefore there are still more questions than answers in this field. Some of the most pressing problems of the field (from our point of view) are listed below.

1. The nature of the barrier in both grain boundary and *c*-axis junctions is unknown. In the better studied case of grain boundary junctions, we believe that the barrier is in the tunnel limit and for sufficiently large misorientation angles there are no pinholes in it. However, the typical barrier width and height don't seem to be well known. Therefore also the impact angle dependence of the barrier transmission is not known a priori. On the other hand, in order to explain the current-phase relation of 45° grain boundary junctions, we had to assume a weak impact angle dependence. It remains to be seen whether this agrees with the barrier properties determined independently, e.g. making use of the STM microscopy where the junction is viewed from above along a path crossing the grain boundary. With such a method, both the barrier height and width could be measurable.

2. The role of various types of disorder in the junction region (interface roughness and faceting, spatially fluctuating barrier height and width, etc.) has to be studied systematically. In particular, disorder is believed to reduce the ability of 45° grain boundary junctions to support mid-gap states [39] and therefore diminishes the second harmonic as well. On the other hand, simple symmetry arguments predict a suppression of the first harmonic of  $I(\varphi)$  by the surface roughness. Also an explicit calculation of the first harmonic in the presence of a finite barrier roughness supports this conclusion [40]. A reliable answer to the question about which of the above two effects of disorder dominates is therefore crucial in order to decide whether disorder increases the ratio of the second and first harmonics of the current-phase relation  $|I_2/I_1|$  as suggested in Section 4, or it rather diminishes it. If the latter alternative is realized, then the experimental observation of a large second harmonic provides even stronger argument in favour of anomalous quantum phase fluctuations in the (bulk) cuprates.

3. Interface roughness and disorder in the barrier region may be also responsible for the weak impact angle dependence of the barrier transmission, which is implied by the large second harmonics observed in 45° grain boundary junctions.

4. From the point of view of applications, especially the grain boundary Josephson junctions have attracted a lot of interest recently. In particular, junctions with sufficiently large second harmonics support doubly degenerate ground states (see Fig. 16) and it has

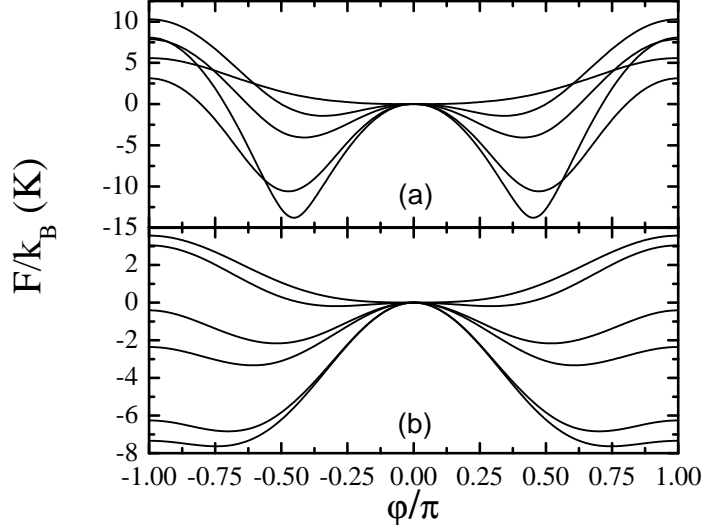


Figure 16: Free energy  $F(\varphi)$  as a function of the phase difference across the weak link (taken from [4]). The zero of energy has been set so that  $F(0) = 0$ . (a) Asymmetric  $45^\circ$  grain boundary. Top to bottom curves correspond to  $T = 40, 30, 20, 15, 10$ , and  $4.2$  K, respectively. (b) Symmetric  $45^\circ$  grain boundary. Top to bottom curves correspond to  $T = 20, 15, 11, 10, 5$ , and  $1.6$  K, respectively.

been suggested [53] that this property might be exploited in the construction of a ‘quiet qubit’, i.e. of a two level system which couples only weakly to its environment and can be used as a basic element in a quantum computer. This is a fascinating proposal and a lot of efforts is being spent on its realization. Several nontrivial problems have to be solved before the final goal can be reached: on the technological side, a technique for a reproducible fabrication of well behaved submicron grain boundary junctions has to be developed. From the point of view of basic science, new routes to reducing the coupling of the junction to the environment are to be looked for, in order to make the junctions really quiet.

## ACKNOWLEDGEMENTS

We thank M. H. S. Amin, A. Golubov, H. E. Hoenig, R. P. J. IJsselsteijn, Z. Ivanov, S. Kashiwaya, P. V. Komissinski, M. Yu. Kupriyanov, S. A. Kovtonyuk, H.-G. Meyer, A. N. Omelyanchouk, G. A. Ovsyannikov, V. Schultze, Y. Tanaka, N. Yoshida, A. M. Zagoskin, and V. Zakosarenko for collaborations on solving the problems discussed in this paper. We learned a lot also from discussions with Yu. S. Barash, V. Bezák, M. V. Fistul, H. Hilgenkamp, R. Kleiner, J. Mannhart, R. G. Mints, A. Plecenik, N. Schopohl, M. Sigrist, and A. Y. Tzalenchuk. R. H. and M. G. were supported by the Slovak Scientific Grant Agency under Grant No. VEGA-1/9177/02 and by the Slovak Science and Technology Assistance Agency under Grant No. APVT-51-021602. E. I. was supported by DFG (Ho461/3-1). The support by D-Wave Systems is also acknowledged.

## REFERENCES

- [1] K. K. Likharev, *Rev. Mod. Phys.* 51 [1979] 101.
- [2] C. C. Tsuei and J. R. Kirtley, *Rev. Mod. Phys.* 72 [2000] 969.
- [3] E. Il'ichev, V. Zakosarenko, R. IJsselsteijn, H. E. Hoenig, V. Schultze, H.-G. Meyer, M. Grajcar, and R. Hlubina, *Phys. Rev. B* 60 [1999] 3096.
- [4] E. Il'ichev, M. Grajcar, R. Hlubina, R. P. J. IJsselsteijn, H. E. Hoenig, H.-G. Meyer, A. Golubov, M. H. S. Amin, A. M. Zagorskin, A. N. Omelyanchouk, and M. Y. Kupriyanov, *Phys. Rev. Lett.* 86 [2001] 5369.
- [5] P. V. Komissinski, E. Il'ichev, G. A. Ovsyannikov, S. A. Kovtonyuk, M. Grajcar, R. Hlubina, Z. Ivanov, Y. Tanaka, N. Yoshida, and S. Kashiwaya, *Europhys. Lett.* 57 [2002] 585.
- [6] M. Grajcar, R. Hlubina, E. Il'ichev, and H.-G. Meyer, *Physica C* 368 [2002] 267.
- [7] H. Hilgenkamp and J. Mannhart, *Rev. Mod. Phys.* 74 [2002] 485.
- [8] E. Il'ichev, V. Zakosarenko, R. P. J. IJsselsteijn, V. Schultze, H.-G. Meyer, H. Hoenig, and H. Töpfer, *IEEE Trans. on Appl. Supercond.* 9 [1999] 3994.
- [9] M. B. Walker and J. Luettmmer-Strathmann, *Phys. Rev. B* 54 [1996] 588.
- [10] M. Sigrist and T. M. Rice, *J. Phys. Soc. Jpn.* 61 [1992] 4283.
- [11] Y. Tanaka, *Phys. Rev. Lett.* 72 [1994] 3871.
- [12] J. Mannhart, H. Hilgenkamp, B. Mayer, C. G. J. R. Kirtley, K. A. Moler, and M. Sigrist, *Phys. Rev. Lett.* 77 [1996] 2782.
- [13] C. R. Hu, *Phys. Rev. Lett.* 72 [1994] 1526.
- [14] A. J. Millis, *Phys. Rev. B* 49 [1994] 15408.
- [15] J. Y. T. Wei, N.-C. Yeh, D. F. Garrigus, and M. Strasik, *Phys. Rev. Lett.* 81 [1998] 2542.
- [16] L. Alff, S. Kleefisch, U. Schoop, M. Zittartz, T. Kemen, T. Bauch, A. Marx, and R. Gross, *Eur. Phys. J. B* 5 [1998] 423.
- [17] H. Walter, W. Prusseit, R. Semerad, H. Kinder, W. Assmann, H. Huber, H. Burkhardt, D. Rainer, and J. A. Sauls, *Phys. Rev. Lett.* 80 [1998] 3598.
- [18] Y. Tanaka and S. Kashiwaya, *Phys. Rev. B* 53 [1996] R11957.
- [19] S. Kashiwaya and Y. Tanaka, *Rep. Prog. Phys.* 63 [2000] 1641.
- [20] T. Löfwander, V. S. Shumeiko, and G. Wendin, *Supercond. Sci. Technol.* 14 [2001] R53.

- [21] Y. S. Barash, Phys. Rev. B 61 [2000] 678.
- [22] A. Huck, A. van Otterlo, and M. Sigrist, Phys. Rev. B 56 [1997] 14163.
- [23] M. Sigrist, Prog. Theor. Phys. 99 [1998] 899.
- [24] M. H. S. Amin, A. N. Omelyanchuk, and A. M. Zagoskin, Phys. Rev. B 63 [2001] 212502.
- [25] T. Löfwander, V. S. Shumeiko, and G. Wendin, Phys. Rev. B 62 [2000] R14653.
- [26] K. A. Kouznetsov, A. G. Sun, B. Chen, A. S. Katz, S. R. Bahcall, J. Clarke, R. C. Dynes, D. A. Gajewski, S. H. Han, M. B. Maple, J. Giapintzakis, J.-T. Kim, and D. M. Ginsberg, Phys. Rev. Lett. 79 [1997] 3050.
- [27] A. G. Sun, A. Truscott, A. S. Katz, R. C. Dynes, and B. W. Veal, Phys. Rev. B 54 [1996] 6734.
- [28] R. Kleiner, A. S. Katz, A. G. Sun, R. Summer, D. A. Gajewski, S. H. Han, S. I. Woods, E. Dantsker, B. Chen, K. Char, M. B. Maple, R. C. Dynes, and J. Clarke, Phys. Rev. Lett. 76 [1996] 2161.
- [29] M. Sigrist, K. Kuboki, P. A. Lee, A. J. Millis, and T. M. Rice, Phys. Rev. B 53 [1996] 2835.
- [30] R. Haslinger and R. Joynt, J. Phys.:Condens. Matter 12 [2000] 8179.
- [31] C. O'Donovan, M. D. Lumsden, B. D. Gaulin, and J. P. Carbotte, Phys. Rev. B 55 [1997] 9088.
- [32] H. J. H. Smilde, Ariando, D. H. A. Blank, G. J. Gerritsma, H. Hilgenkamp, and H. Rogalla, Phys. Rev. Lett. 88 [2002] 057004.
- [33] R. G. Mints, Phys. Rev. B 57 [1998] R3221.
- [34] N. Miyakawa, J. F. Zasadzinski, L. Ozyuzer, P. Guptasarma, D. G. Hinks, C. Kendziora, and K. E. Gray, Phys. Rev. Lett. 83 [1999] 1018.
- [35] J. Halbritter, Phys. Rev. B 46 [1992] 14861.
- [36] R. Hlubina, cond-mat/0210516.
- [37] G. Deutscher, Nature 397 [1999] 410.
- [38] Y. I. Latyshev, T. Yamashita, L. N. Bulaevskii, M. J. Graf, A. V. Balatsky, and M. P. Maley, Phys. Rev. Lett. 82 [1999] 5345.
- [39] M. Matsumoto and H. Shiba, J. Phys. Soc. Jap. 64 [1995] 1703.
- [40] Y. S. Barash, H. Burkhardt, and D. Rainer, Phys. Rev. Lett. 77 [1996] 4070.
- [41] R. Rifkin and B. Deaver, Phys. Rev. B 13 [1976] 3894.



- [42] E. Il'ichev, V. Zakosarenko, L. Fritzsche, R. Stolz, H. E. Hoenig, H.-G. Meyer, M. Götz, A. B. Zorin, V. V. Khanin, A. B. Pavolotsky, and J. Niemeyer, *Rev. Sci. Instr.* 72 [2001] 1882.
- [43] H. Hilgenkamp and J. Mannhart, *Appl. Phys. Lett.* 73 [1998] 265.
- [44] F. V. Komissinskii, G. A. Ovsyannikov, N. A. Tulina, and V. V. Ryazanov, *Sov. Phys.-JETP* 89 [1999] 1160.
- [45] Y. Tanaka and S. Kashiwaya, *Phys. Rev. Lett.* 74 [1995] 3451.
- [46] W. E. Pickett, *Rev. Mod. Phys.* 61 [1989] 433.
- [47] T. Xiang and J. Wheatley, *Phys. Rev. Lett.* 77 [1996] 4632.
- [48] E. L. Wolf, *Principles of Electron Tunneling Spectroscopy*. Oxford University Press, New York [1985].
- [49] Z. X. Shen and D. Dessau, *Physics Reports* 253 [1995] 1.
- [50] A. V. Zaitsev, *Sov. Phys.-JETP* 59 [1984] 1015.
- [51] N. Didier, C. Dubourdieu, A. Rosová, B. Chenevier, V. Galindo, and O. Thomas, *J. of Alloys and Compounds* 251 [1997] 322.
- [52] S. L. Cooper and K. E. Gray, In D. M. Ginsberg, editor, *Physical Properties of High Temperature Superconductors IV*. World Scientific, Singapore [1994].
- [53] L. B. Ioffe, V. B. Geshkenbein, M. V. Feigel'man, A. L. Fauchère, and G. Blatter, *Nature* 398 [1999] 679.